Comparative Analysis of the Secretome from a Model Filarial Nematode (*Litomosoides sigmodontis*) Reveals Maximal Diversity in Gravid Female Parasites*[S]

Stuart D. Armstrong‡, Simon A. Babayan§§§, Nathaly Lhermitte-Vallarino¶, Nick Gray§, Dong Xia‡, Coralie Martin¶, Sujai Kumar§¶¶, David W. Taylor‖, Mark L. Blaxter§, Jonathan M. Wastling‡, and Benjamin L. Makepeace‡‡‡**

Filarial nematodes (superfamily Filarioidea) are responsible for an annual global health burden of ~6.3 million disability-adjusted life-years, which represents the greatest single component of morbidity attributable to helminths affecting humans. No vaccine exists for the major filarial diseases, lymphatic filariasis and onchocerciasis; in part because research on protective immunity against filariae has been constrained by the inability of the human-parasitic species to complete their lifecycles in laboratory mice. However, the rodent filaria *Litomosoides sigmodontis* has become a popular experimental model, as BALB/c mice are fully permissive for its development and reproduction. Here, we provide a comprehensive analysis of excretory-secretory products from *L. sigmodontis* across five lifecycle stages and identifications of host proteins associated with first-stage larvae (microfilariae) in the blood. Applying intensity-based quantification, we determined the abundance of 302 unique excretory-secretory proteins, of which 64.6% were present in quantifiable amounts only from gravid adult female nematodes. This lifecycle stage, together with immature microfilariae, released four proteins that have not previously been evaluated as vaccine candidates: a predicted 28.5 kDa filaria-specific protein, a zonadhesin and SCO-spondin-like protein, a vitellogenin, and a protein containing six metridin-like ShK toxin domains. Female nematodes also released two proteins derived from the obligate *Wolbachia* symbiont. Notably, excretory-secretory products from all parasite stages contained several uncharacterized members of the transthyretin-like protein family. Furthermore, biotin labeling revealed that redox proteins and enzymes involved in purinergic signaling were enriched on the adult nematode cuticle. Comparison of the *L. sigmodontis* adult secretome with that of the human-infective filarial nematode *Brugia malayi* (reported previously in three independent published studies) identified differences that suggest a considerable underlying diversity of potential immunomodulators. The molecules identified in *L. sigmodontis* excretory-secretory products show promise not only for vaccination against filarial infections, but for the amelioration of allergy and autoimmune diseases. *Molecular & Cellular Proteomics 13: 10.1074/mcp.M114.038539, 2527–2544, 2014.*

Filarial nematodes are the most important helminth parasites of humans in terms of overall impact on public health, with an annual global burden of ~6.3 million disability-adjusted life-years (1). Lymphatic filariasis (LF)[1] or "elephantiasis," which affects populations across Africa, South Asia, the Pacific, Latin America, and the Caribbean, accounts for 92% of this toll. The remainder is caused by onchocerciasis or "river blindness," primarily in sub-Saharan Africa. The major human filarial pathogens are *Wuchereria bancrofti* (responsible for 90% of LF cases), *Brugia malayi* and *Brugia timori* (geographically restricted causes of LF), and *Onchocerca volvulus* (the sole agent of human onchocerciasis). In addition, *Loa loa* affects ~13 million people in West and Central Africa. This parasite usually induces a relatively mild disease, but has been associated with severe and sometimes fatal adverse

From the ‡Institute of Infection and Global Health, University of Liverpool, Liverpool L3 5RF, UK; §Centre for Immunity, Infection & Evolution and Institute of Evolutionary Biology, University of Edinburgh, Edinburgh EH9 3JT, UK; ¶UMR 7245 MCAM CNRS, Muséum National d'Histoire Naturelle, 75231 Paris, France; ‖Division of Pathway Medicine, University of Edinburgh, Edinburgh EH9 3JT, UK; **The National Institute for Health Research, Health Protection Research Unit in Emerging and Zoonotic Infections, University of Liverpool, Liverpool L3 5RF, UK

Received, February 13, 2014, and in revised form, June 4, 2014
Published, MCP Papers in Press, June 23, 2014, DOI 10.1074/mcp.M114.038539
Author contributions: S.D.A., S.A.B., C.M., D.W.T., M.L.B., J.M.W., and B.L.M. designed research; S.D.A., S.A.B., N.L.V., and N.G. performed research; S.D.A., D.X., S.K., M.L.B., and B.L.M. analyzed data; S.D.A., S.A.B., M.L.B., and B.L.M. wrote the paper.

[1] The abbreviations used are: LF, lymphatic filariasis; gAF, gravid adult female; pgAF, pre-gravid adult female; AM, adult male; iMf, immature microfilariae; bMf, blood-derived microfilariae; vL3, vector-derived L3; ESP, excretory-secretory products; WBE, whole body extracts; *w*Ls, *Wolbachia* endosymbiont of *Litomosoides sigmodontis*; TTL, transthyretin-like; CPI, cysteine proteinase inhibitor.

events following anthelmintic chemotherapy (2). Filarial parasites are primarily drivers of chronic morbidity, which manifests as disabling swelling of the legs, genitals and breasts in LF; or visual impairment and severe dermatitis in onchocerciasis. The filariae are also a major problem in small animal veterinary medicine, with ~0.5 million dogs in the USA alone infected with *Dirofilaria immitis* (3), the cause of potentially fatal heartworm disease. However, in domesticated ungulates, filarial infections are generally benign (4).

Currently, control of human filarial diseases is almost entirely dependent on three drugs (ivermectin, diethylcarbamazine, and albendazole). Prevention of heartworm also relies on prophylactic treatment of dogs and cats with ivermectin or other macrocyclic lactones. Reports of possible ivermectin resistance in *O. volvulus* (5) and *D. immitis* (6) have highlighted the importance of maintaining research efforts in vaccine development against filarial nematodes. However, rational vaccine design has been constrained for several decades (7) by the intrinsic complexity of these metazoan parasites and their multistage lifecycle. Moreover, many filarial species carry obligate bacterial endosymbionts (*Wolbachia*), which may also stimulate the immune response during infection (8). As part of global efforts to improve prevention and treatment of these diseases, large-scale projects have been undertaken, including sequencing of the nematodes (9–11) and their *Wolbachia* (10, 12, 13), and proteomic analyses of both whole organisms and excretory-secretory products (ESP) (14, 15). Additionally, two studies (both on *B. malayi*) have examined lifecycle stage-specific secretomes (16, 17). In the context of vaccine design, the identification of ESP proteins and determination of their expression in each major lifecycle stage can facilitate the prioritization of candidates for efficacy screening in animal models.

One barrier to the progression of research in the filarial field is our inability to maintain the full lifecycle of the human parasites in genetically tractable hosts. This lifecycle involves uptake of the first-stage larvae (microfilariae, Mf) by a hematophagous arthropod and two moults in the vector, followed by transmission of third-stage larvae (L3) to a new vertebrate host and two further moults before the nematodes mature as dioecious adults. However, the complete lifecycle of the New World filaria *Litomosoides sigmodontis* can be maintained in laboratory rodents, including inbred mice (18). This species [incorrectly referred to as *L. carinii* in the older literature (19)] was first studied in its natural host, the cotton rat (*Sigmodon hispidus*) (20). Mongolian jirds (*Meriones unguiculatus*) are also fully permissive for *L. sigmodontis* infection and are routinely used for maintaining its lifecycle in the laboratory, as they tolerate higher parasite burdens than do laboratory mice. To exploit the full power of murine immunology, including defined knockout strains, *L. sigmodontis* in mice has been used to address questions regarding the fundamental immunomodulatory mechanisms employed by filarial parasites (21, 22), their ability to mitigate proinflammatory pathology and autoimmune disease (23), and the impact of various vaccine strategies on adult nematode burden and fecundity (24, 25).

Using the resource of a newly-determined genome sequence, coupled with a derivative of the intensity-based absolute quantification (iBAQ) proteomic approach, we have examined the stage-specific secretome of *L. sigmodontis* in vector-derived L3 (vL3), adult males (AM), pre-gravid adult females (pgAF), gravid adult females (gAF), and immature Mf (iMf). In addition to identifying dynamic changes in the ESP profile through the lifecycle, we show important differences in the adult secretomes of *L. sigmodontis* and *B. malayi*, especially in the abundance of two novel proteins released by female *L. sigmodontis* that lack orthologs in *B. malayi*. As has been observed in other parasitic nematodes, we find transthyretin-like family (TTL) proteins to be particularly dominant in the ESP. Active expulsion of uterine fluid may account for the remarkable diversity of proteins that we detect in gAF ESP, and we highlight several novel proteins that warrant evaluation in vaccine trials and as anti-inflammatory mediators.

EXPERIMENTAL PROCEDURES

Ethical Considerations—All experimental procedures on the animals required for vL3 production at the Muséum National d'Histoire Naturelle were approved by the ethical committee "Cuvier" (n° 68–002) and carried out in strict accordance with EU Directive 2010/63/UE and the relevant national legislation (French Décret n° 2013–118, 1 February 2013). All other parasite stages were harvested from animals maintained at the University of Edinburgh in compliance with a UK Home Office Animals (Scientific Procedures Act) 1986 project license and the recommendations of the local ethical review committee.

Parasites and Protein Preparations—The life cycle of *L. sigmodontis* was maintained in jirds infected with vL3 harvested from the mite vector *Ornithonyssus bacoti*. After 70 - 90 days, gAF and AM were recovered from the pleural cavity by lavage with serum-free RPMI 1640 medium (Invitrogen, Carlsbad, CA), whereas pgAF were recovered 32 days postchallenge. To harvest iMf liberated *in vitro*, gAF culture medium was removed after 24 h and centrifuged at 1900 × *g* for 20 min (4 °C). Blood-derived microfilariae (bMf) were obtained by overlay of blood (from cardiac puncture of jirds >75 days post-infection) onto a 25% Percoll suspension, centrifugation at 1900 × *g* for 20 min (4 °C), and passage of the bMf fraction through a PD-10 desalting column (GE Healthcare) prior to culture. The vL3 larvae were dissected directly from the mite vector and washed three times in RPMI 1640 before transfer to culture vessels.

To determine the relative abundance of proteins in the secretome of each parasite stage, ESP and whole body extracts (WBE) were extracted and analyzed separately. Parasites were incubated in serum-free RPMI 1640 supplemented with 100 U/ml penicillin, 100 μg/ml streptomycin, and 1% glucose at 37 °C (5% CO_2) in ultra-low attachment flasks (Corning), and were confirmed to be viable during incubation by microscopic examination. The medium was replaced every 24 h, and spent media recovered at 24 h and 48 h were centrifuged at 1900 × *g* for 20 min (4 °C) in low protein-binding Oak Ridge tubes (polypropylene copolymer; Thermo Scientific Nalgene) to remove debris. To purify proteins from the supernatant, hydroxylated silica slurry (StrataClean Resin, Agilent Technologies, Santa Clara, CA) was added at 30 μl/ml and vortex-mixed at high speed for 2 min. Resin used for each 24 h incubation sample was reused for the respective 48 h sample to concentrate ESP prior to storage at −80 °C. Initial experiments using soluble WBE (used as a proxy for

ESP, as limited amounts of the latter were available) displayed no visible differences in protein profiles by SDS-PAGE using resin-bound protein compared with equivalent unbound material (data not shown). Analyses were performed with separate ESP batches in quadruplicate for gAF, triplicate for AM, and duplicate for pgAF, iMf, and vL3.

Soluble WBE was prepared by homogenization in 25 mM ammonium bicarbonate, 1% *Rapi*Gest SF surfactant (Waters), and cOmplete Protease Inhibitor Mixture (Roche) using a mini-pestle in a microcentrifuge tube. This was followed by 10 cycles of sonication on ice using a Vibra-Cell VCX130PB sonicator (Sonics & Materials, Inc., Newtown, CT) with microprobe (10 s sonication alternating with 30 s incubation on ice). Homogenized samples were centrifuged at 13,000 × *g* for 20 min (4 °C) and the supernatant retained. The WBE preparations were obtained from single pools of parasites for all stages except gAF and AM, where two biological replicates were available. Protein concentrations were determined using the Pierce Coomassie Plus (Bradford) Protein Assay (Thermo Scientific).

Surface Biotinylation of Live Worms—Samples of 10 adult male and five female nematodes were washed three times with pre-chilled PBS buffer and incubated for 30 min with 1 mM EZ-link Sulfo-NHS-SS-Biotin (Thermo scientific), or PBS only (negative control), at 4 °C with gentle agitation. The biotinylating solution was removed, and the reaction quenched with 100 mM glycine in PBS before washing the nematodes three times in PBS-glycine. Labeled nematodes were stored at −80 °C. Surface proteins were extracted by sequential incubations in PBS buffer alone, 1.5% octyl β-D-glucopyranoside (Sigma), 0.5% SDS and then 4 M urea (all in PBS) for 1 h each (room temperature). Proteins released at each step were incubated with 30 μl of high-capacity streptavidin-agarose beads (Thermo Scientific) for 2 h at room temperature with rotary mixing. To recover bound biotinylated proteins, the supernatant was removed and the beads were washed three times in PBS and three times in 25 mM ammonium bicarbonate prior to incubation in 50 mM DTT (Sigma), 25 mM ammonium bicarbonate at 50 °C for 30 min. The supernatant was removed and the DTT diluted 10-fold before digestion with 0.2 μg proteomic-grade trypsin (Sigma) overnight at 37 °C. The resultant peptides were concentrated using C_{18} reverse-phase spin filters (Thermo Scientific) according to the manufacturer's instructions prior to MS analysis.

To confirm efficient and specific labeling of the parasite surface, AM and gAF were fixed in 70% hot ethanol after subjection to biotin and control labeling as above. Paraffin-embedded sections (4 μm) were deparaffinized, rehydrated and blocked in 1% BSA and 0.3% Triton X-100 in PBS (blocking buffer) for 1 h (room temperature), followed by two 5-min washes in PBS with gentle agitation. The sections were incubated with streptavidin-FITC (Sigma) at a 1/1000 dilution in blocking buffer for 1 h (room temperature), washed three times, and mounted with ProLong Gold anti-fade reagent (Invitrogen). Images were obtained on an Axio Imager.M2 fluorescence microscope (Zeiss, Oberkochen, Germany) using Zen 2012 software (Zeiss), combining the FITC channel with brightfield illumination.

Sample Preparation for Proteomics—StrataClean Resin containing bound ESP was washed twice with 25 mM ammonium bicarbonate before suspension in 0.1% RapiGest SF and 25 mM ammonium bicarbonate. The resin samples were heated at 80 °C for 10 min, reduced with 3 mM DTT at 60 °C for 10 min, cooled, then alkylated with 9 mM iodoacetamide (Sigma) for 30 min (room temperature) protected from light. All steps were performed with intermittent vortex-mixing. The samples were then digested using 0.2 μg proteomic-grade trypsin at 37 °C overnight with rotation, centrifuged at 13,000 × *g* for 5 min, and the supernatant removed. The resin was washed twice with 0.1% *Rapi*Gest SF, 25 mM ammonium bicarbonate, and the supernatants pooled. To remove *Rapi*Gest SF, the samples were precipitated using TFA (final concentration, 1%) at 37 °C for 2 h and centrifuged at 12,000 × *g* for 1 h (4 °C). The peptide supernatant was concentrated using C_{18} reverse-phase spin filters according to the manufacturer's instructions. The WBE samples were reduced and alkylated as above, digested with trypsin at a protein/trypsin ratio of 50:1 at 37 °C overnight, and precipitated to remove *Rapi*Gest SF as for the ESP preparations.

NanoLC MS ESI MS/MS Analysis—Peptide solutions (2 μl) were analyzed by on-line nanoflow LC using the nanoACQUITY-nLC system (Waters) coupled to an LTQ-Orbitrap Velos (Thermo Scientific) MS equipped with the manufacturer's nanospray ion source. The analytical column (nanoACQUITY UPLC BEH130 C_{18} 1.7 μm particle size, 15 cm × 75 μm capillary column) was maintained at 35 °C and a flow-rate of 300 nl/min. The gradient consisted of 3%-40% ACN, 0.1% formic acid for 45 or 90 min, then a ramp of 40%-85% ACN, 0.1% formic acid for 3 min in positive ionization mode. Full scan MS spectra (*m/z* range 300 - 2000) were acquired by the Orbitrap at a resolution of 30,000, and analysis was performed in data-dependent mode. The top 20 most intense ions from MS1 scan (full MS) were selected for tandem MS by CID and all product spectra were acquired in the LTQ ion trap. Ion trap and Orbitrap maximal injection times were set to 50 ms and 500 ms, respectively.

Thermo RAW files were imported into Progenesis LC-MS (version 4.1, Nonlinear Dynamics, Newcastle upon Tyne, UK). Where necessary, technical replicate (repeat injection) runs were time-aligned using default settings and an auto-selected run as a reference. Peaks were picked by the software using default settings and filtered to include only peaks with a charge state between +2 and +6. Peptide intensities of technical replicates were normalized against the reference run by Progenesis LC-MS. Spectral data were transformed to MGF files with Progenesis LC-MS and exported for peptide identification using the Mascot (version 2.3.02, Matrix Science, Boston, MA) search engine. Tandem MS data were searched against translated ORFs from the *L. sigmodontis* genome and its *Wolbachia* symbiont, *w*Ls [obtained from http://nematodes.org/genomes/litomosoides_sigmodontis, release nLs 2.1.2, 10,246 protein sequences (M. Blaxter, S. Kumar, G. Koutsovoulos; unpublished); and release *w*Ls 2.0, 1042 protein sequences (26)], together with predicted proteomes for the rodent host (*Mus musculus*, Uniprot release 2012_08, 16,626 protein sequences; and *Meriones unguiculatus*, Uniprot release 2012_08, 223 protein sequences) and a general contaminant database (GPMDB, cRAP version 2012.01.01, 115 protein sequences). Search parameters included a precursor mass tolerance of 10 ppm, a fragment mass tolerance of 0.5 Da, and allowance for one missed tryptic cleavage. Carbamidomethylation (cysteine) was set as a fixed modification and oxidation (methionine) set as a variable modification. Mascot search results were further validated using the machine learning algorithm Percolator embedded within Mascot. The Mascot decoy database function was utilized and the false discovery rate was <1%, whereas individual percolator ion scores >13 indicated identity or extensive homology ($p < 0.05$). Mascot search results were imported into Progenesis LC-MS as XML files and analyzed according to the following criteria: at least two unique peptides were required for reporting protein identifications, and an individual protein had to be present in ≥two biological replicates to be included in the ESP data set. Protein abundance was calculated by the iBAQ method; that is, the sum of all peak intensities (from Progenesis output) divided by the number of theoretically observable tryptic peptides (27). Protein abundance was normalized by dividing the protein iBAQ value by the summed iBAQ values for the corresponding sample, and the reported abundance is the mean of the biological replicates. Normalized peptide intensities rather than iBAQ values were used to calculate fold-changes between control and biotinylated worm surface preparations. Mass spectrometric data have been deposited in the

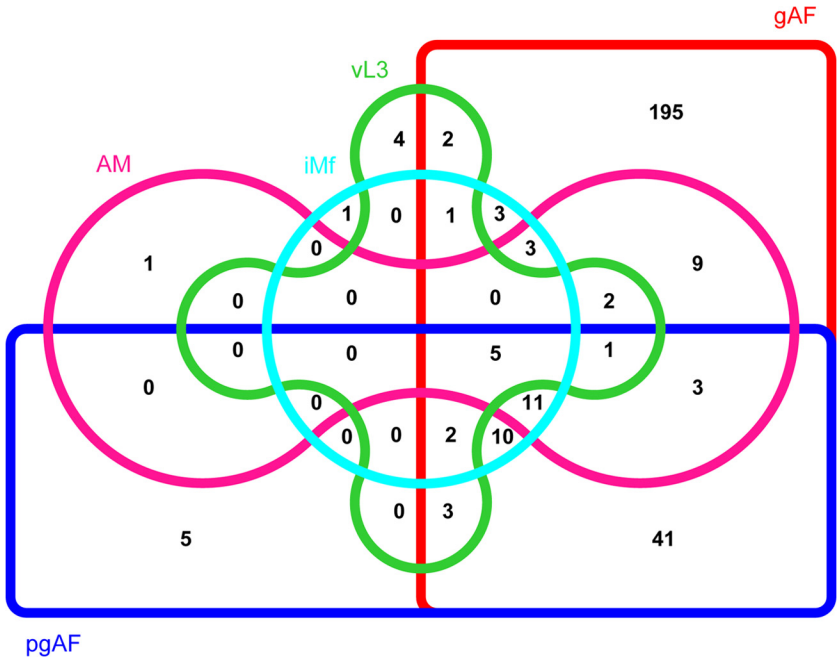

FIG. 1. **Distribution of ESP proteins between life stages of *L. sigmodontis*.** Venn diagram of the shared and stage-specific ESP proteins in each of the life stages examined.

ProteomeXchange Consortium database (http://proteomecentral.proteomexchange.org) via the PRIDE partner repository (28) with the dataset identifier PXD000756 and DOI 10.6019/PXD000756.

In Silico Analyses of Proteins—The domain content of proteins identified in the ESP was assessed using Pfam (v. 27.0) with the gathering threshold as a cut-off. A hypergeometric test for enrichment of Pfam domains in ESP proteins compared with the complete predicted proteome of *L. sigmodontis* was performed using the phyper toolkit within the R programming environment (29). The Benjamini & Hochberg step-up FDR-controlling procedure was applied to the calculated, adjusted *p* values (30). Structural homologs of abundant uncharacterized proteins were identified through comparison to the National Center for Biotechnology Information non-redundant protein database (delta-blast search; E-value cut-off 1^{-03}) and to the UniProt database (psi-blast search) *via* the Phyre^2 protein fold recognition server (31). The conserved domain structure of selected, abundant ESP proteins was also interrogated in InterProScan 4 (32). Venn diagrams were created using vennture (33), whereas for heat-maps, hierarchical cluster analysis was performed using the (1 - *r*) distance metric in gene-e (http://www.broadinstitute.org/cancer/software/GENE-E). Prediction of classical N-terminal signal peptides, non-classical secretion signatures, mitochondrial targeting sequences, *O*-glycosylation sites, and propeptide cleavage sites was performed using the SignalP 4.0 server (34), the SecretomeP 2.0 server (35), MitoProt (36), the NetOGlyc 4.0 server (37), and the ProP 1.0 server (38), respectively. *Brugia malayi* orthologs of *L. sigmodontis* proteins were determined using reciprocal blast with a bit score cut-off of 50.

ShK domains were identified in the complete predicted proteomes of the filariae *B. malayi* (9), *D. immitis* (10), *L. sigmodontis*, *Onchocerca ochengi, Acanthocheilonema viteae* (draft unpublished genomes available at http://www.nematodes.org/genomes/; Blaxter et al., unpublished), *W. bancrofti,* and *L. loa* (11), plus the ascaridid nematode *Ascaris suum* (39) (which is an outgroup for the filarial species), using the Pfam hidden Markov model for the domain and hmmer (version 3.1b.1). Each domain was excised and a total of 531 distinct domains identified, which were aligned using ClustalOmega (40). Inspection of the alignment revealed that a subset of domains were misaligned (and therefore did not have the six cysteine residues in register with the others); these were corrected manually. The alignment was analyzed for phylogenetic signal using MrBayes (version 3.2) (41) and two runs of four chains each were run for two million generations. The first million generations were discarded as burn-in after inspection in Tracer (version 1.5; A. Rambaut, unpublished: http://tree.bio.ed.ac.uk/software/tracer/) and a consensus tree was inferred from the remaining 10,000 samples taken every 100 generations. Sequence logos were generated for all 531 ShK domains, all domains from nLs_04059 and orthologs, and each of the six distinct sets of orthologous domains, using the WebLogo server (http://weblogo.berkeley.edu/) (42).

RESULTS

Distribution of Proteins in ESP Across Parasite Lifecycle Stages—We searched ~120,000 MS spectra per lifecycle stage against protein sequences predicted from the *L. sigmodontis* and *w*Ls genome assemblies. A total of 302 quantifiable filarial proteins (*i.e.* represented by ≥2 unique peptides in ≥2 biological replicates) were detected in ESP across the five lifecycle stages. A majority of these (195 proteins, 64.6%) were uniquely identified in gAF (Fig. 1, supplemental Fig. S1). Hierarchical clustering of the proteomic profiles clearly separated ESP and WBE (Fig. 2). The vL3 ESP data profile was distinct; not only from that of the other ESP preparations, but also from vL3 WBE (Fig. 2). The closer clustering of iMf with pgAF ESP rather than gAF ESP was surprising, but may reflect the much lower complexity of the pgAF and iMf ESP datasets. Strikingly, excluding gAF, fewer than six stage-specific proteins each were observed in ESP (Table I). In vL3, these included highly expressed vaccine candidates originally identified from L3 of other filarial species, including activation-associated secreted protein 1 (ASP-1) and abundant larval transcript protein 1 (ALT-1). The functional identities of proteins restricted to other lifecycle stages were unexpected.

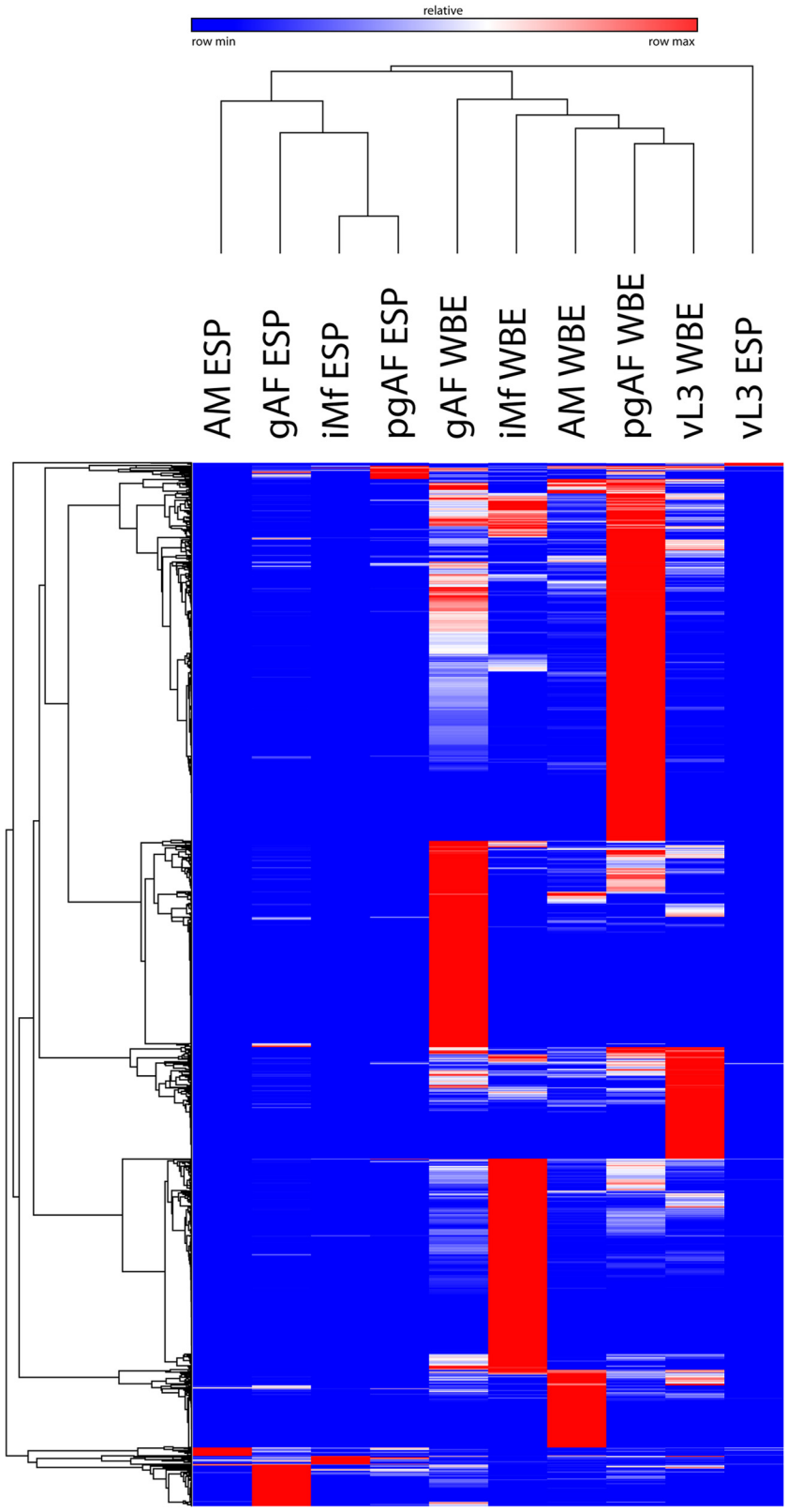

FIG. 2. **Heat-map of protein profiles for ESP and WBE of *Litomosoides sigmodontis*.** Dendrograms were generated by hierarchical clustering based on pair-wise distance.

TABLE I

Proteins unique to the excretory-secretory products of individual lifecycle stages of Litomosoides sigmodontis. ESP, excretory-secretory products; pgAF, pre-gravid adult female; AM, adult male; vL3, vector-derived third-stage larvae; iMf, immature microfilariae

Parasite stage ESP[a]	Locus tag	Annotation
pgAF	nLs_02441	Epicuticlin
	nLs_07093	Nucleoredoxin-like protein-2
	nLs_03968	Nematode cuticle collagen N-terminal domain containing protein
	nLs_06052	Translationally controlled tumor protein
	nLs_00526	Glutathione reductase
AM	nLs_07249	Glutaredoxin-like protein
vL3	nLs_06400	Activation-associated secreted protein-1
	nLs_09374	Abundant larval transcript-1 protein
	nLs_03087	Cathepsin L-like precursor
	nLs_06524	Calmodulin
iMf	nLs_02254	MSP domain-containing protein

[a] Data for excretory-secretory products unique to gravid adult females are not shown due to the large number of proteins (195) in this category (see supplemental Table S1).

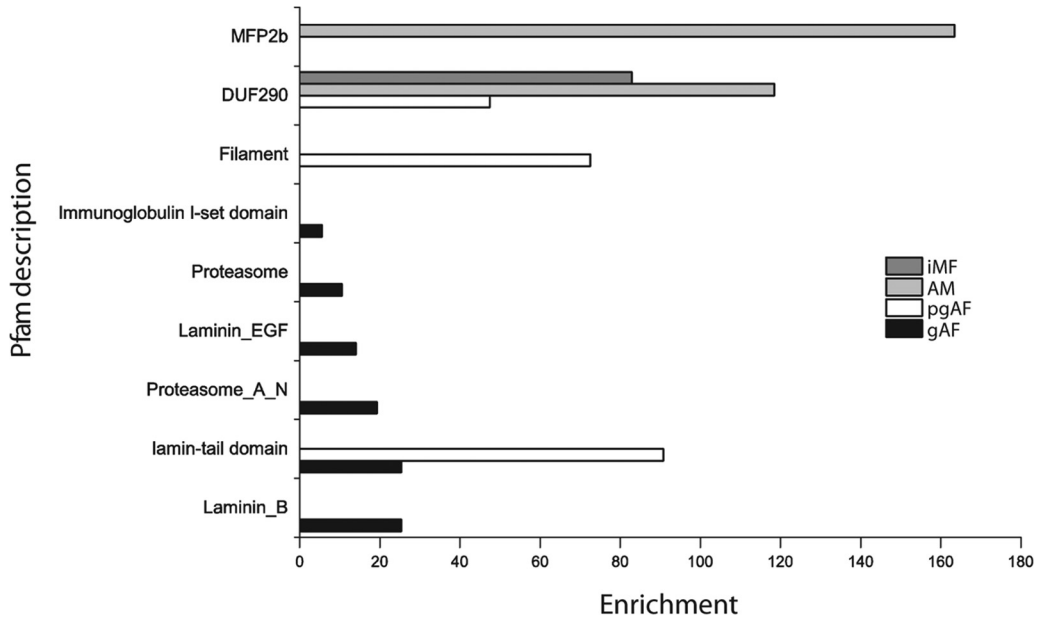

FIG. 3. **Pfam enrichment analysis of ESP proteins against the complete theoretical proteome of *L. sigmodontis*.** The fold-enrichment is displayed for each lifecycle stage; DUF290 represents the transthyretin-like protein family.

Thus, pgAF released two cuticular proteins and two antioxidant proteins that were not observed in ESP from gAF (Table I). The only *w*Ls-derived proteins that were quantifiable in any ESP were two components of the GroELS chaperonin complex, which were found solely in preparations from pgAF and gAF (supplemental Table S1).

We explored functional distinctness of ESP from different lifecycle stages by determining protein domain overrepresentation relative to the complete predicted proteome of *L. sigmodontis*. The greatest fold-enrichment scores were observed in the AM ESP, which contained three proteins with a major sperm protein (MSP) fiber protein 2b (MFP2b) domain and 10 proteins with the TTL family domain, "DUF290" (Fig. 3). The TTL family was also overrepresented in iMf (seven proteins) and pgAF (nine proteins). Notably, pgAF exhibited significant enrichment for intermediate filament and lamin-tail domains (three members each). The ESP from gAF was enriched for lamin-tail and immunoglobulin I-set domains, as well as two proteasome and two laminin families (Fig. 3). To evaluate specifically the propensity of individual proteins to be enriched in ESP relative to WBE, we plotted iBAQ values from the ESP datasets against the WBE datasets for each lifecycle stage. Overall, iMf, AM and pgAF secreted a greater proportion of proteins with relatively low abundance in WBE than did vL3 and gAF (Fig. 4). However, all of the lifecycle stages exhibited secretomic profiles clearly distinct from WBE, in that proteins which were highly abundant in ESP tended to be rare in WBE and *vice-versa* (Fig. 5, supplemental Fig. S2). Identification of proteins in ESP was strongly correlated with sequence features suggesting secretion: 31.1% of ESP protein sequences were predicted to begin with a classical signal peptide, whereas a further 30.5% were predicted to contain

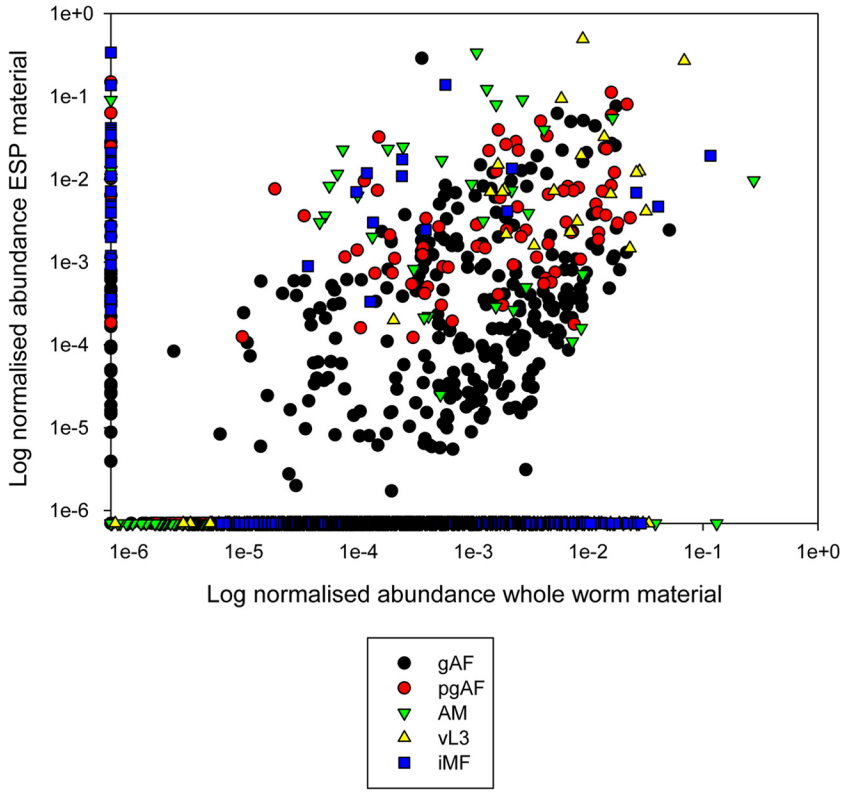

FIG. 4. **Relative abundance of *L. sigmodontis* ESP proteins compared with corresponding WBE.** ESP proteins (≥2 peptides detected at $p < 0.05$ and <1% FDR, present in ≥2 biological replicates) were quantified by ion intensity (iBAQ) and compared with the iBAQ abundance of the same protein present in nematode WBE (*x* axis). Individual abundance values were normalized by dividing by the summed total abundance of that individual sample (life stage). The normalized abundance ratio was used as a guide to evaluate the enrichment of the protein. Note that as the data are normalized within each life stage, direct comparisons of abundance between them is not valid.

an internal, non-classical secretion signature (supplemental Table S1).

Abundant Proteins Released by Adult Parasites—The gAF ESP displayed the most complex composition. Functionally defined components of the ESP included a small cysteine proteinase inhibitor [CPI (43)], the omega-class glutathione *S*-transferases [GST (44)], the MSPs (45), and the microfilarial sheath protein (46) (Fig. 5*B*). Additionally, *L. sigmodontis* homologs of Av33 and ES-62, proteins known to be abundant in the ESP from adult females of other filarial species, were identified. Av33 is similar to an aspartate protease inhibitor from *A. suum* (47), whereas ES-62 is a secreted leucyl aminopeptidase (48). Three of the gAF ESP proteins had putative lipid-binding regions: ML-domain proteins have been reported to interact with cholesterol and lipid A (49, 50), the conserved filarial antigen Ov16 has a putative phosphatidylethanolamine-binding domain (51), and a novel and highly abundant vitellogenin (nLs_07321) contained an amino-terminal lipid transport domain. However, the majority of the abundant proteins secreted by this stage were uncharacterized or contained conserved domains associated with very limited functional information (Fig. 5*B*). The dominant gAF ESP protein (nLs_03577) was unique to filarial nematodes, exhibiting only very weak similarity to a bacterial P-type ATPase (supplemental Tables S2 and S3). Other salient proteins from gAF ESP included twelve distinct TTL family proteins (Fig. 5*B*) and an abundant protein (nLs_08836), also well-represented in pgAF and iMf ESP, which contained von Willebrand factor type-d (VWD) and cysteine-rich (C8) domains in its carboxy-terminal portion. The best match identified for nLs_08836 was an apolipophorin from *A. suum*, but nLs_08836 lacks the expected amino-terminal lipoprotein domain, and the carboxy-terminal portion displayed weak similarity to predicted zonadhesin-like or SCO-spondin proteins (supplemental Tables S2 and S3). A protein that contained six metridin-like ShK toxin domains, nLs_04059, was moderately abundant in gAF ESP and was also observed in pgAF, AM, and iMf secretomes (Fig. 5, supplemental Figs. S2*B* and S3). Although the ShK domain has a wide phylogenetic distribution, the particular pattern apparent in nLs_04059 is limited to filariae (supplemental Tables S2 and S3; see below for detailed analyses of this protein). Several proteins present in gAF ESP [RAL-2 (52), SXP-1 (53), S3 (54), and CCG-1 (55)] were homologs of previously described ESP antigens from filariae or other parasitic nematodes, but remain functionally obscure.

Despite extensive overlap in the identities of the most abundant ESP proteins across the parasite lifecycle (Fig. 1, supplemental Fig. S1), several molecules were overrepresented in individual stages. In pgAF, abundant proteins included several glycolytic enzymes and two heat-shock proteins, as well as a galectin (β-galactoside-binding protein 1) and a highly unusual protein, nLs_03350, containing both C-type lectin and acetylcholine receptor domains (Fig. 5*C*). A secreted acid phosphatase, which may be involved in riboflavin metabolism and have a role in the hydrolysis of prosthetic groups such as flavin mononucleotide and/or pyridoxal 5-phosphate (56, 57),

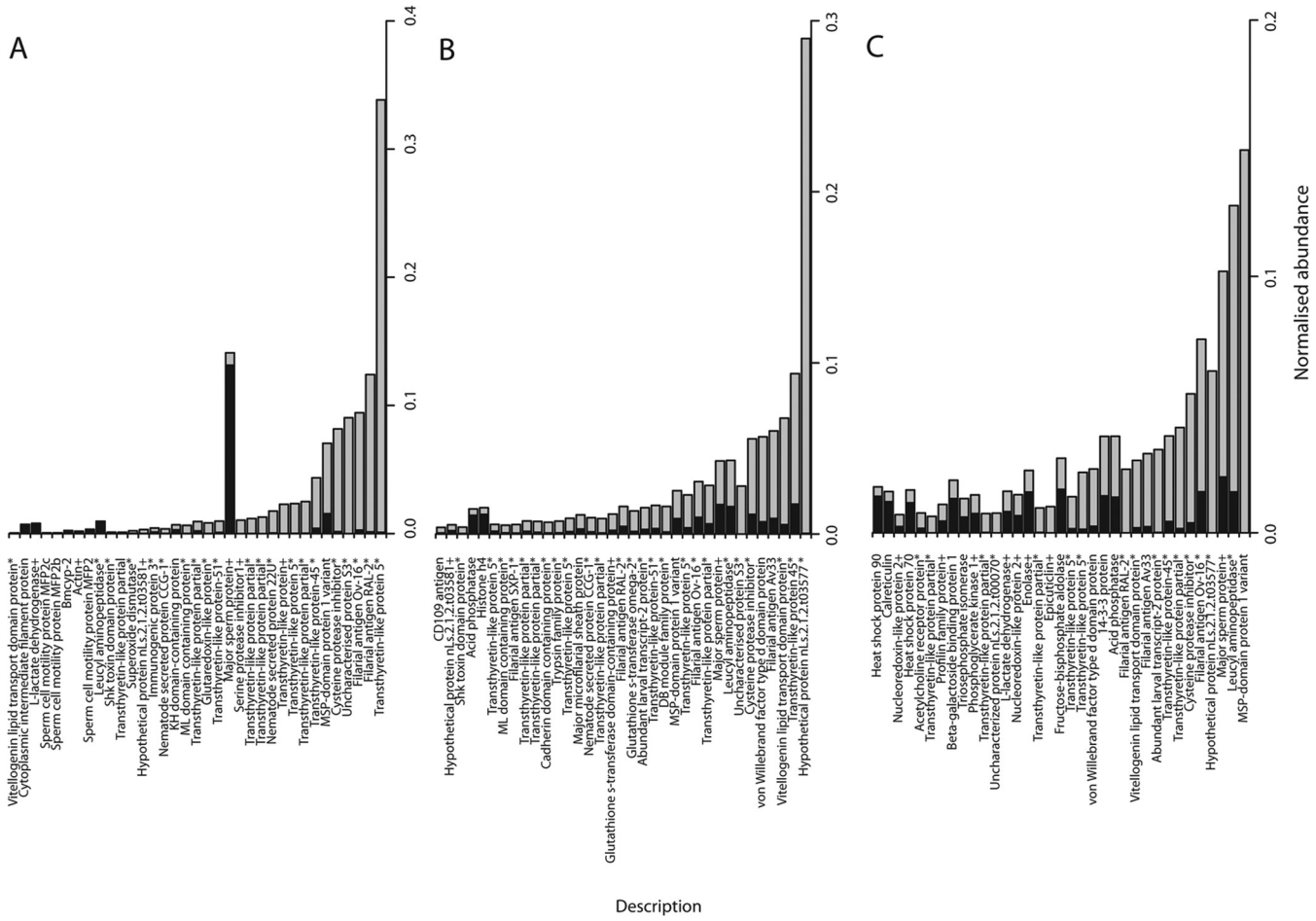

FIG. 5. **Comparison of ESP protein abundance (iBAQ) in adult stages of *L. sigmodontis*.** The top 35 most abundant proteins in each ESP (*A*, AM; *B*, gAF; *C*, pgAF) are ranked by normalized iBAQ abundance (gray bars); the corresponding abundance in WBE is displayed for comparison (black bars) in stacked format. Individual protein abundance values were normalized by the summed total abundance per sample. An asterisk indicates proteins with a predicted signal peptide, whereas predicted secretion through the nonclassical pathway is indicated by a plus sign.

was also prominent in pgAF ESP (Fig. 5*C*). Abundant components of AM ESP included three isoforms of MFP2 (58) and proteins known to be highly expressed in sperm or seminal fluid, such as an extracellular superoxide dismutase (59) and a serine protease inhibitor (60) (Fig. 5*A*). However, AM ESP also contained several previously described but uncharacterized proteins, such as RAL-2 (52), nematode secreted protein 22U (61), and immunogenic protein 3 (62). A novel KH (RNA-binding) domain protein had homologs in other filarial species, but also displayed weak homology to the Vasa DEAD-box helicase GLH-2 from *Caenorhabditis elegans* (supplemental Table S2), which is associated with spermatogenic chromatin (63).

Abundant Proteins Released by Larval Parasites—Characterization of ESP from the bMf stage posed special challenges. Despite the two-stage purification process and prolonged culture *in vitro*, 92.4% (61 of 66) of proteins robustly quantified in bMf ESP were derived from the rodent host (supplemental Table S4). To characterize Mf-derived ESP in more depth, we harvested iMf from gAF cultures *in vitro*, separated them from the female nematodes, and proceeded with *in vitro* incubation. This procedure increased the detection of proteins of nematode origin to 36 (supplemental Fig. S2*B*), although as expected, the dominant proteins in iMf ESP closely mirrored the profile of gAF ESP (Fig. 5*B*). The vL3 ESP was the least diverse dataset in our study, and was composed largely of previously characterized filarial proteins that are known to be uniquely expressed or enriched in this stage (supplemental Fig. S2*A*).

Phylogenetics of Novel, Filaria-specific ESP Proteins—The most abundant protein in gAF ESP, nLs_03577, was an enigmatic, uncharacterized molecule with a predicted MW of 28.5 kDa and a lack of conserved domains, with the exception of a classical N-terminal signal peptide. Downstream of the signal peptide, moderate to high levels of sequence conservation were apparent across the Filarioidea in the amino-terminal portion (supplemental Fig. S4). However, the carboxy-terminal segment displayed low complexity and was highly variable

between filariae, whereas two isoforms in *B. malayi* diverged only in this region (supplemental Fig. S4). The *L. sigmodontis* protein was predicted to contain six potential *N*-linked and 11 *O*-linked glycosylation sites, as well as propeptide cleavage sites at positions 31 and 147. The former cleavage site was absolutely conserved within the Filarioidea, despite some variation in the motif, whereas the latter (at position 154 of the consensus) was unique to *L. sigmodontis*. These observations suggest that several processed isoforms of nLs_03577 might be secreted by *L. sigmodontis*. Phylogenetic analysis of nLs_03577 orthologs confirmed that this protein is restricted to the Filarioidea, with no representatives in *A. suum* or other non-filarial nematodes. The base of the tree was poorly resolved because of the lack of signal in the carboxy-terminal portion (supplemental Fig. S5). However, nLs_03577 clearly clustered with an ortholog in the rodent filaria, *A. viteae*, whereas orthologs in *D. immitis* and *Onchocerca* spp. formed the most distant grouping (supplemental Fig. S5).

The ShK domain protein nLs_04059 was a particularly distinctive molecule identified in all ESP preparations except vL3. One other *L. sigmodontis* ShK domain protein, the astacin protease nLs_03368, was a rare component of gAF ESP only (supplemental Table S1). The ShK domain (or metridin-like toxin domain, also known as the SXC or six-cysteine domain) was first identified in cnidarian venoms, but is particularly abundant in nematode proteomes (64), where it is associated with secreted proteins. The prototypic ShK peptide (from the cnidarian *Stichodactyla helianthus*) is a type 1 toxin that blocks voltage-gated potassium channels, and synthetic analogs are currently under development as a therapy for autoimmune diseases, in which Kv1.3 channels expressed by effector memory T-lymphocytes are specifically targeted (65). Although nLs_04059 was not especially abundant in any single ESP preparation, its presence in the secretomes of all mammalian-derived stages and its unusual domain structure (supplemental Fig. S3) suggest a potentially immunomodulatory role.

The nLs_04059 protein has the largest number of ShK domains (six) of any protein in *L. sigmodontis*. We identified orthologous genes in all of the other filarial genomes, each containing six ShK domains (supplemental Fig. S6). The nLs_04059-like ShK domains formed a distinct subset of all filarial and *A. suum* ShK domains (supplemental Fig. S6 and S7), with a striking pattern of conservation, particularly around the last three universally-conserved cysteine residues (Fig. 6). A proline residue (at position 32 of the alignment, but residue 17 of the nLs_04059 domains) was also strongly conserved in the nLs_04059 domains (Fig. 6), but not common in the full set of 531 domains. In nLs_04059 and its orthologs, the six ShK repeats are separated by five low-complexity spacers (27–104 amino acids) (Supplemental Fig. S3). Some spacer domains were conserved, but others showed variation in the pattern and length of low complexity, serine-rich regions. These have no clear similarity to other proteins, but by analogy to the ShK mucins of the ascaridid *Toxocara canis* (66), they could be recipients of *O*-linked glycan decorations. Although there are 65 potential *O*-glycosylation sites on nLs_04059, we found that it migrated exclusively at the expected molecular weight of the unmodified mature protein (~52 kDa) by geLC MS, ruling out a mucin-like structure (data not shown). This protein also contained two lysyltyrosine dyads located within the carboxy-terminal ShK domain (Supplemental Fig. S3). Because a lysyltyrosine dyad is essential for binding of type-1 cnidarian peptide toxins to potassium channels (67), this could be related to Kv1 channel-blocking activity. Notably, one lysyltyrosine dyad in ShK domain 6 is conserved in many (although not all) orthologs in other species (Fig. 6).

Proteins Associated with the Adult Nematode Surface—The nematode cuticle is the critical interface between the parasite and the immune system of its host (68). Surface-associated proteins may simply mirror ESP, perhaps by passive adsorption of released material, or comprise a distinct component of the exoproteome. Live AM and gAF nematodes were surface-labeled incubated with Sulfo-NHS-SS-Biotin and fractionated. We identified five proteins present in biotin-labeled AM extracts and 11 proteins in biotin-labeled gAF (Table II) that were absent in unlabeled controls. In addition, a further four (AM) and 39 (gAF) proteins were enriched by more than 50-fold in biotin-labeled samples relative to unlabeled controls (supplemental Table S5), suggesting that these molecules were abundant on the parasites' surface but may also be associated with endogenous biotin. Accordingly, fluorescent imaging of fixed nematode sections confirmed that biotin labeling was largely confined to the cuticular layers (supplemental Fig. S8), although low levels of endogenous biotin were present within internal structures. There was considerable overlap between ESP and biotin-labeled protein profiles in both sexes. However, AM and gAF displayed two and 12 proteins, respectively, that were uniquely present in surface-labeled extracts (Table II, supplemental Table S5). Conversely, many of the highly abundant ESP proteins, such as nLs_03577, the vitellogenin nLs_07321, uncharacterized protein S3, and ES-62 were not detected in biotin-labeled extracts.

A striking feature of the surface-associated proteins was the presence of two ectoenzymes involved in purinergic signaling. These were an adenylate kinase predominant in AM extracts and a purine nucleoside phosphorylase found exclusively found in gAF extracts (69) (Table II and supplemental Table S5). A homolog of complement component 1, q subcomponent-binding protein was identified in gAF surface-labeled extracts. Like the human homolog, the *L. sigmodontis* protein contained an N-terminal mitochondrial import signal sequence, although the former is expressed in a number of extramitochondrial locations, including on the surface of lymphocytes, endothelial cells, dendritic cells, and platelets (70). These proteins may play a role in immunomodulation, as purinergic signaling is known to regulate lymphocyte traffick-

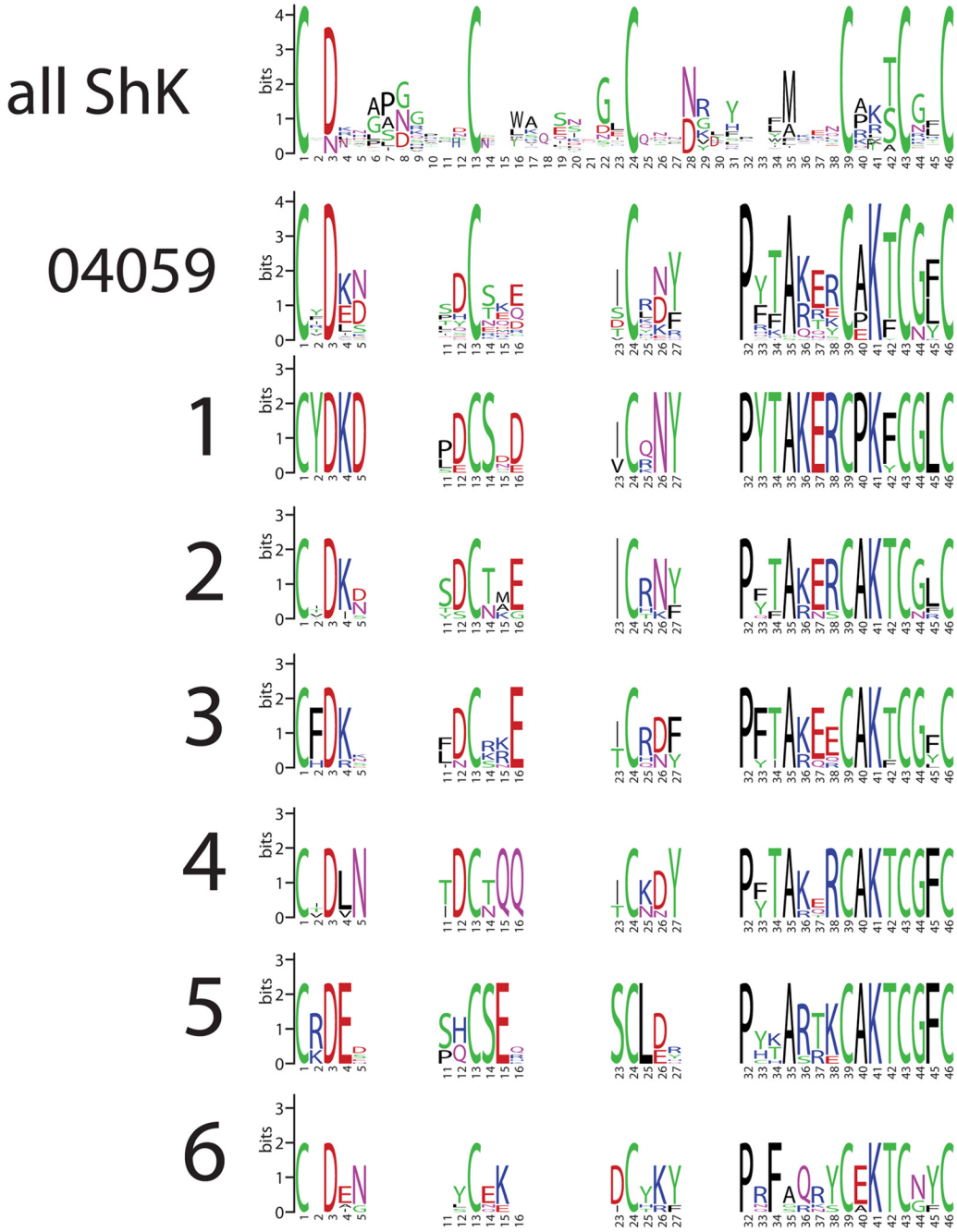

FIG. 6. **The ShK domains from *L. sigmodontis* protein nLs_04059 and its orthologs in other filarial species have a distinct sequence signature.** All ShK domains identified in the complete theoretical proteomes of *L. sigmodontis, B. malayi, L. loa, W. bancrofti, O. ochengi, D. immitis, Acanthocheilonema viteae* and *Ascaris suum* were extracted and aligned, and sequence logos derived from: (all ShK) all 531 domains, (04059) all domains from nLs_04059 and its orthologs, (1–6) the aligned orthologous domains 1 through 6 from nLs_04059 and its orthologs. No nLs_04059 ortholog was found in *A. suum.* As the nLs_04059 domains are relatively short, there are gaps in the sequence logos for the nLs_04059-derived domains. Numbering in all panels is based on the full ShK alignment.

ing (69), whereas the complement component 1q receptor is involved in vasodilation via the generation of bradykinin (70).

Surface extracts from AM contained a homolog of the actin-binding protein, calponin, which has been localized to both striated muscle and the cuticle in adult *O. volvulus* (71). The gAF surface extracts contained two proteins, protein disulfide isomerase and a leucine-rich repeat family protein, both of which have previously been associated with cuticle synthesis in filariae and *C. elegans* (72, 73). Stress response-related proteins were also well represented on gAF [including thioredoxin peroxidase (74), aldehyde dehydrogenase, a thioredoxin-like protein and heat-shock proteins], as were several

TABLE II

Putative surface-associated proteins detected in biotin-labelled adult worm whole body extracts that were absent from unlabelled controls. ESP, excretory-secretory products; AM, adult male; OG, octyl β-D-glucopyranoside; gAF, gravid adult female; FMN, flavin mononucleotide

Parasite stage	Treatment	Peptides used for quantitation	Confidence score	Locus tag	Annotation	Presence in ESP
AM	OG	7	857.06	nLs_06907	Adenylate kinase isoenzyme 1	No
	OG	4	417.27	nLs_09715	Major sperm protein	Yes
	OG	2	186.68	nLs_01742	Filarial antigen Av33	No
	OG	2	297.13	nLs_08458	Filarial antigen Ov16	Yes
	SDS	2	308.12	nLs_07359	Calponin actin-binding domain containing protein	No
gAF	OG	2	233.80	nLs_09095	Protein disulphide isomerase	No
	SDS	2	86.22	nLs_08755	Leucine-rich repeat family protein	No
	SDS	3	118.56	nLs_09715	Major sperm protein	Yes
	SDS	2	99.43	nLs_02353	Complement component 1, q subcomponent-binding, mitochondrial-like	No
	SDS	2	61.97	nLs_01344	Thioredoxin peroxidase 1	No
	SDS	2	108.87	nLs_07321	Vitellogenin	Yes
	PBS	2	309.24	nLs_00851	DNA repair protein Rad4-containing protein	Yes
	PBS	2	309.24	nLs_07061	Heat shock 70 kDa protein	Yes
	PBS	2	309.24	nLs_09360	FMN-binding domain protein	No
	PBS	3	463.79	nLs_01364	Transthyretin-like protein, partial	Yes
	PBS	2	309.24	nLs_03263	Thioredoxin domain-containing protein	Yes

enzymes of pyruvate metabolism (Table II and supplemental Table S5). Notably, the endosymbiont-derived *Wolbachia* surface protein was found to be accessible to surface biotinylation in gAF.

Comparison with the Secretomes of Adult B. malayi and D. immitis—The ESP from several lifecycle stages of *B. malayi* have been described previously (14, 16, 17), but the only common stage between these studies was adults [with both sexes cultured together in (14)]. Of 297 proteins identified in adult *L. sigmodontis* ESP, 86.9% had an ortholog in the *B. malayi* genome; however, the majority (159) were not observed in the *B. malayi* secretome (Fig. 7*A*). Analysis of Pfam domains failed to indicate any significant enrichment in this unique dataset (data not shown). Conversely, although each *B. malayi* study revealed a surprising number of laboratory-specific secreted proteins, orthologs of the proteins reported in all three *B. malayi* secretomes were also detected in adult *L. sigmodontis* ESP (Fig. 7*A*). This common core included leucyl aminopeptidase, enolase, triosephosphate isomerase, β-galactoside-binding protein 1, acetylcholine receptor protein, cyclophilin-5, and macrophage migration inhibitory factor-1.

The 22 *L. sigmodontis* adult ESP proteins that lacked *B. malayi* orthologs (Fig. 7*B*) included two of the most highly abundant gAF ESP molecules (the vitellogenin nLs_07321 and the VWD protein nLs_08836), together with secretory protein Ls110 and two superoxide dismutase isoforms. Although the *B. malayi* secretome studies identified a total of 90 proteins that did not have orthologs in *L. sigmodontis* (Fig. 7*B*), only one (cuticular glutathione peroxidase) was observed in all three studies. Because standardized quantification methods were not used for our *L. sigmodontis* and the published *B. malayi* studies, it is difficult to determine whether adult *B. malayi* and *L. sigmodontis* differ in their levels of secretion for individual ESP proteins. However, in terms of rank abundance, triosephosphate isomerase, macrophage migration inhibitory factor-1, and γ-glutamyl transpeptidase were reported to be grossly overrepresented in adult *B. malayi*; whereas adult *L. sigmodontis* ESP was enriched for uncharacterized protein nLs_03577 (orthologous to Bm1_38495), TTL protein nLs_09750 (orthologous to Bm1_43635), and homologs of Av33 and S3 (supplemental Table S1). Proteins that were apparently equally abundant in relative terms between each species included leucyl aminopeptidase and homologs of CPI-2 and Ov16.

We are aware of only a single large-scale study on the secretome of canine heartworm (*D. immitis*), which identified 110 proteins from mixed adult worm cultures (75). Of these, 86.4% had an ortholog in the *L. sigmodontis* genome, but only 43.2% of the *D. immitis* orthologs were present in the adult *L. sigmodontis* secretome (Fig. 7*C*). This is similar to the degree of overlap previously observed between *D. immitis* and *B. malayi* ESP profiles (75). Importantly, most of the proteins identified in the common core between *L. sigmodontis* and *B. malayi* were also present within the set shared by *L. sigmodontis* and *D. immitis*, although the latter included a greater number (nine) of TTL family members. Moreover, the abundant *L. sigmodontis* gAF ESP components that were absent or apparently scarce in the *B. malayi* datasets (uncharacterized protein nLs_03577, vitellogenin nLs_07321, and the VWD protein nLs_08836) were not detected in *D. immitis* ESP (supplemental Table S1). As reported by Geary et al. (75), *D. immitis* ESP contained several proteins that might be associated with the release of microvesicles, including exocyst complex component-2, α-actinin, RhoGAP domain-containing proteins, and several transcription factors. Orthologs of these proteins were not detected

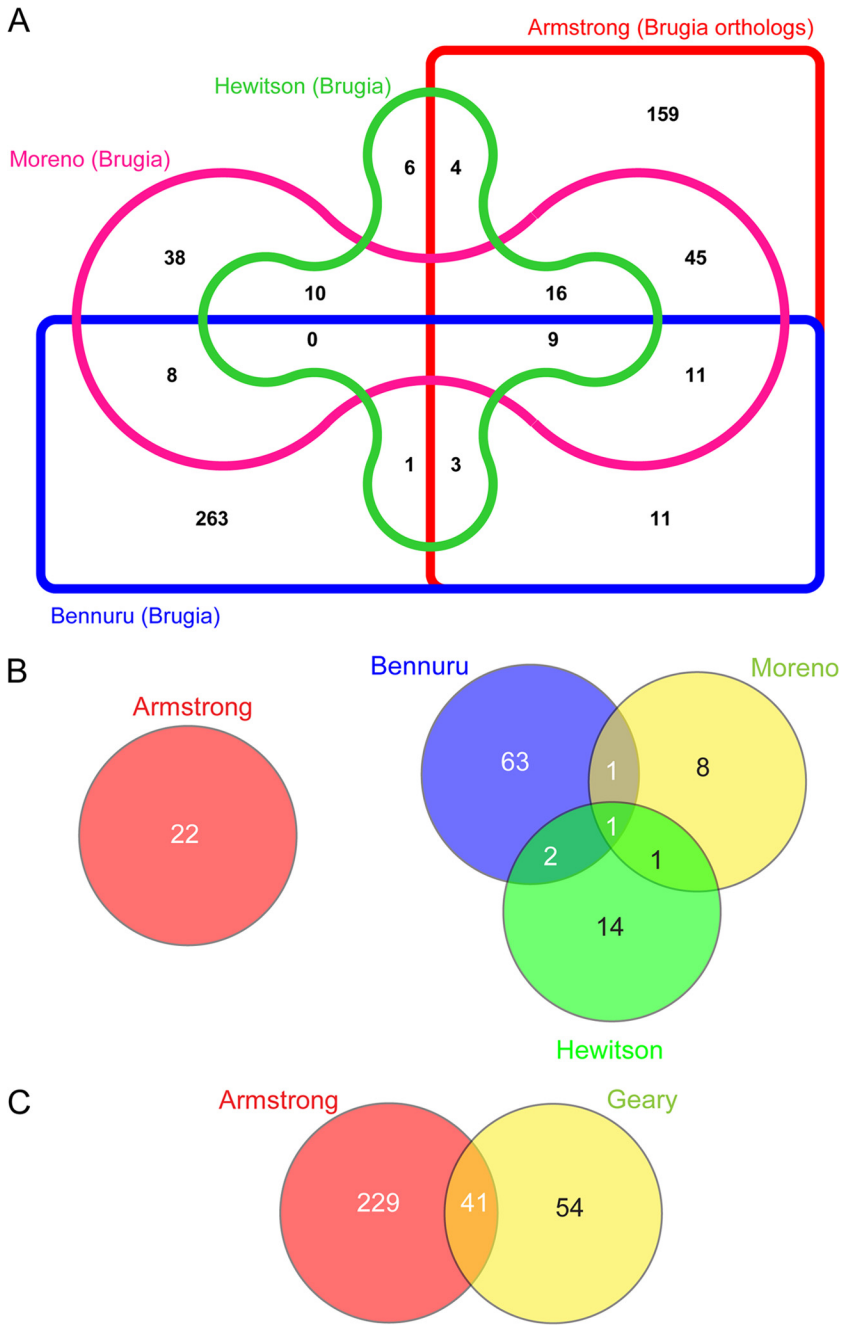

FIG. 7. **Number of adult ES proteins detected in published studies of *B. malayi* and *D. immitis* adults and comparisons with orthologs present in the *L. sigmodontis* adult secretome.** The study-specific and shared proteins represent combined data from both adult sexes. Note that protein identifications are those quoted by each individual study and statistical cut-offs have not been standardized. *Brugia malayi* and *D. immitis* orthologs of *L. sigmodontis* proteins were identified by reciprocal BLAST of the respective theoretical proteomes (bit score >50). The distribution of the orthologs in adult nematode ESP across *L. sigmodontis* ("Armstrong") and previously published studies is displayed for *A*, *B. malayi* (14, 16, 17) and *C*, *D. immitis* (75), whereas *B*, summarizes the distribution of species-specific (non-orthologous) proteins for *L. sigmodontis* and *B. malayi*.

in *L. sigmodontis* ESP, perhaps indicating a distinct role for microvesicles in the biology of heartworm.

DISCUSSION

Quantifying the Secretomes of a Model Filarial Nematode—Filarial nematodes exact a significant burden of morbidity in human populations and are important pathogens of companion animals. Although efficacious anti-filarial drugs exist, the spectre of the evolution of genetic resistance to these is ever-present (5, 6), and alternative routes to treatment are required. In addition to treating patent disease, it would be highly desirable to prevent infection, and thus an anti-filarial vaccine would be an extremely valuable addition to current medical and veterinary chemotherapeutic options (76). The ESP released by parasites into their hosts have been the target of vaccine development for decades, but the understanding of these molecules in filarial nematodes is limited. Whereas previous studies have cataloged the proteins inferred to be present in filarial ESP, quantitative assessments of their abundance have not been explored previously using an intensity-based approach.

In *L. sigmodontis*, gAF was responsible for the majority of ESP proteomic diversity. The other four lifecycle stages ex-

amined contributed only 11 proteins (3.6% of the total) that were not present in gAF ESP. This finding contrasts with a qualitative analysis of *B. malayi* secretomes comparing adults, Mf and L3, and incorporating data obtained from single-peptide hits, which found that Mf contributed the greatest proportion of unique proteins (17). However, an earlier assessment of the *B. malayi* gAF, AM and Mf secretomes concluded that gAF produced the greatest number of unique hits (16), suggesting that methodological differences may underlie these contrasting results. The diversity of gAF ESP is consistent with the material containing not only somatic adult ESP, but also proteins released from the reproductive tract that derive from the processes of oogenesis, fertilization, and embryonic development *in utero* (all filarial pathogens are ovoviviparous).

Nematode sperm are acutely sensitive to aerobic damage (77). The AM ESP contained proteins suggestive of roles in protection of sperm against oxidants and other stressors, including superoxide dismutase, a serine protease inhibitor and a glutaredoxin-like protein. Glutaredoxins are thiol-containing antioxidant proteins, and *C. elegans* GLRX-21 plays a key role in mitigating selenium toxicity (78). Mammalian seminal fluid accumulates selenium, which if in excess, can impede sperm motility (79). A homolog of the serine protease inhibitor is secreted by *A. suum* during the acquisition of motility and contributes to sperm competition by inhibiting the activation of surrounding spermatids (80). Lysis of sperm during aerobic culture may account for the high levels of MSPs observed in AM ESP and in ESP obtained from pgAF, gAF, and iMf. Female nematodes are fertilized some weeks before the first Mf are produced (81), and the dominance of MSPs in pgAF ESP indicates that leakage of sperm from the female reproductive tract occurs before parturition.

Several unique antioxidant proteins (nucleoredoxin-like protein-2, glutathione reductase, and translationally-controlled tumor protein) were found in pgAF ESP, suggesting an enhanced requirement for protection during this stage. In *B. malayi*, homologs of the nucleoredoxin-like proteins, which resemble large thioredoxins (82), are present in ESP but do not exhibit stage-specific expression (83). Two unique cuticle biosynthesis-related proteins were also released by pgAF, suggesting that cuticular remodeling occurs during their final stages of growth. This may result in increased susceptibility to immune-driven oxidative stress or damage during copulation (84). Heat-shock proteins, which were overrepresented in pgAF ESP, have been detected in *B. malayi* adult nematode ESP (85).

The Abundant Uncharacterized Proteins Released by Gravid Adult Female Nematodes—We identified four abundantly secreted or excreted proteins, found predominantly in gAF and iMf ESP, that had not been reported previously. Two have only marginal similarity to annotated proteins: nLs_03577, which displayed a significant match to a P-type ATPase (but lacked an ATPase domain), and nLs_08836, which showed some similarity to zonadhesin, a VWD protein located in the head of mammalian sperm (86). However, we note that nLs_08836 is not an ortholog of the *C. elegans* zonadhesin-domain protein, DEX-1 (87). The third novel protein, nLs_07321, is a vitellogenin. In *C. elegans*, vitellogenins are expressed exclusively in the intestine, where they bind cholesterol and transport it via the body cavity to the gonad (88). Subsequently, oocytes internalize the protein and its lipid cargo by receptor-mediated endocytosis and store it in yolk granules (88). Several vitellogenins have also been identified in ESP derived from adults of the oviparous gastrointestinal nematode, *Heligmosomoides polygyrus* (89). The fourth protein, the ShK domain protein nLs_04059, was distinct from other proteins containing this motif in nematodes, both in the number of domains and their specific sequence. Its relative abundance, distinctiveness, and presence in all the filarial species surveyed suggest that it may be a viable vaccine candidate for both human filarial diseases and canine heartworm. Its role *in vivo* may be to interfere with the development of acquired immunity by inhibiting the Kv1 channels of memory T-cells in a manner analogous to the activity of cnidarian ShK toxins (65). We are not aware of any reports of such activity for nematode ShK domain proteins, but future studies should focus on the effects of synthetic peptides from nLs_04059 and its orthologs, or full-length recombinant proteins, on memory T-cell function.[2]

Finally, the uncharacterized TTL family has emerged as one of the most typical and widespread findings in ESP from both zoo- and phytoparasitic nematodes (90). In *C. elegans*, there are 63 TTL genes, many of which are secreted and apparently up-regulated in response to infectious challenge, but only TTR-52 has been ascribed a physiological function [phagocytosis of apoptotic cells (91)]. In the phytoparasite *Radopholus similis, Rs-ttl-2*, which is closely related to one of the most abundant *L. sigmodontis* TTL proteins (nLs_07576; found in ESP from all stages except vL3 in our study), was localized to the ventral nerve cord (92). A second *R. similis* TTL family member, *Rs-ttl-1*, was expressed solely in the vulval region (92), and a homolog of this molecule (nLs_07332) was detected in iMf WBE only. Additionally, in the ruminant parasite *Ostertagia ostertagi*, a TTL family member (Oo-TTL-1) was a major component of ESP and could be immunolocalized to the pseudocoelomic fluid of adult worms (93). In our study, a *L. sigmodontis* homolog of Oo-TTL-1 (nLs_09750) was abundant in all ESP preparations except those of vL3. Determining the function of this large and enigmatic protein family will be challenging, although RNA interference approaches are becoming more tractable for filarial nematodes (94).

Uterine Fluid as a Source of Nematode and Endosymbiont Products—Proteins excreted or secreted from filarial nema-

[2] Whilst this manuscript was in press, Chhabra et al. [doi: 10.1096/fj.14-251967] reported that a peptide derived from a *B. malayi* ShK protein can block native Kv1.3 channels in human T-cells.

todes could be derived from a number of routes. In addition to oral secretions from the esophageal glands and release of fecal material from the anus, nematodes also secrete material from the anterior sensory glands (amphids) (95) and the secretory pore, and may also void material from the genital openings during copulation and release of Mf. In addition, proteins can be liberated from the hypodermis through transcuticular secretion (96), especially during moulting, and exosome release may also be important (97). From our data, we suggest that vulval excretion is the main source of ESP proteins in gAF and pgAF, and that the iMf are coated with proteins secreted by the uterine epithelium. This interpretation is supported not only by the abundance of MSPs and vitellogenin in gAF and pgAF ESP, but by the presence of omega-class secreted GST isoforms exclusively in gAF ESP, which in *O. volvulus* are only produced by embryos at the morula stage (44). Similarly, ESP proteins in the male nematode probably originate primarily from seminal fluid. Immune sera from rodents infected with *A. viteae* react most strongly with male and female gonad tissues, including the fluid channels between developing embryos and on sperm in both the spermatheca and seminal vesicle (98).

The molecular basis of the symbiosis between *Wolbachia* and filarial nematodes has not been firmly established, although roles for the endosymbionts in metabolic supplementation and immune evasion are both supported by gene expression studies (13). It has been proposed that *Wolbachia* may be present in uterine fluid (99), inside degenerating embryos (100), or may exit *via* the secretory pore (101). Additionally, they apparently secrete proteins into structures that lack bacterial cells, such as the cuticle (102). *Wolbachia*-derived proteins were present in very low amounts in *B. malayi* secreted products (17). We identified *Wolbachia* GroELS components in ESP of pgAF and gAF, but not in other lifecycle stages. GroEL is the most abundant protein in *Wolbachia* (13, 15), and its detection in ESP may be through release of whole bacterial cells, for example from the female uterus *via* degenerating oocytes or embryos, or through secretion. GroEL, as a chaperonin, would be expected to be confined to the cytosol, although GroEL homologs have been reported to "moonlight" on the surface of some bacterial species (103). We also detected *Wolbachia* surface protein by surface labeling of adult *L. sigmodontis*, as has been reported in *B. malayi* (102). This protein is a putative ligand of Toll-like receptors 2 and 4 (100), and our finding supports the hypothesis that *Wolbachia* modifies and perhaps misdirects the immune response to filariae (104). Whether *Wolbachia* GroEL also stimulates proinflammatory Toll-like receptors has not been evaluated, but a precedent exists in other bacteria (105), and antibodies against this protein are associated with pathology in LF (106).

The L. sigmodontis Secretome and Vaccine Development for Filariases—Vaccine development for human and veterinary filariases has focused on the L3 stage because irradiated L3 are highly efficacious at inducing long-lasting protective immunity (24, 107, 108) and strong anti-L3 immunity may block parasite establishment. *Litomosoides* is an excellent model for L3 vaccine research, as the L3 expresses a very similar repertoire of genes to the human and veterinary pathogens (109). Our analyses of ESP from *L. sigmodontis* vL3 reinforced our understanding of a stereotypical secretomic profile for this stage. However, no defined parasite antigens (whether alone or in combination) have reproducibly attained an equivalent level of protection to irradiated L3 in any filarial system (7). Furthermore, because a single pair of adult nematodes can generate a patent infection, vaccines directed solely against L3 face a potentially insurmountable challenge.

Targeting of Mf has the potential to block transmission, and in the case of onchocerciasis, to reduce disease pathology. Moreover, the Mf stage has been shown to be more vulnerable to protective immune responses than have L3 in several vaccination trials (110–112). Vaccination with a combination of ALT-1 and CPI-2 delivered as a DNA vaccine reduced circulating Mf levels by up to 90% in *L. sigmodontis*. Importantly, this protection was only achieved if immunomodulatory domains of the antigens were ablated (by mutation or deletion of the coding sequence) and was maintained even when the adult nematode burden was not significantly reduced. This phenomenon was probably because of the immunomodulatory effects of the native (active) proteins, as transplantation of a single adult female worm is sufficient to prevent clearance of injected Mf in naïve hosts (113). We suggest it is likely that many of the other abundant molecules secreted by gAF may similarly have roles in facilitating Mf survival, and could be targeted in an "anti-fecundity" vaccination strategy. Furthermore, the proteins identified by surface labeling of the gAF cuticle may also participate in generating a permissive environment (69, 70); thus, vaccination against these molecules, if sufficiently divergent from host homologs, might impede parasite establishment and transmission.

CONCLUSIONS

We have shown that *L. sigmodontis*, especially the gAF stage, releases a remarkable diversity of proteins into the external milieu and that the majority of these molecules are uncharacterized. Although many of these proteins may be involved in fundamental aspects of embryogenesis, a subset are likely to be active immunomodulatory agents that protect the nematodes (and especially the circulating Mf) from the host immune response. The abundant ESP protein, CPI, may represent an archetype for this dual functionality, as it plays fundamental roles in oogenesis and fertilization not only in parasitic nematodes, but also in *C. elegans* (114). This suggests that its immunomodulatory properties are an example of secondary adaptation to a radically different environment. Thus, the pharmacopeia released by gAF may provide the ideal set of molecular targets for immunoprophylaxis and chemotherapy of filariases; moreover, it could provide new

compounds to tackle proinflammatory and autoimmune diseases (23).

Acknowledgments—We thank Alison Fulton for maintenance of the *L. sigmodontis* lifecycle at the University of Edinburgh, and Stephnie Kennedy for fluorescence imaging of fixed worms at the University of Liverpool.

* This study was supported by the 7th Framework Programme of the European Commission (project identifier HEALTH-F3-2010-242131).

S This article contains supplemental Figs. S1 to S8 and Tables S1 to S5.

‡‡ To whom correspondence should be addressed: Infection Biology, University of Liverpool, Liverpool Science Park IC2, 146 Brownlow Hill, Liverpool, L3 5RF UK. Tel.: 44-151-7941586; Fax: 44-151-7950236; E-mail: blm1@liverpool.ac.uk.

Current addresses §§Institute of Biodiversity, Animal Health and Comparative Medicine, University of Glasgow and Moredun Research Institute, Glasgow G12 8QQ, UK; ¶¶Department of Zoology, University of Oxford, South Parks Road, Oxford, OX1 3PS, UK.

REFERENCES

1. Mathers, C. D., Ezzati, M., and Lopez, A. D. (2007) Measuring the burden of neglected tropical diseases: the global burden of disease framework. *PLoS Negl. Trop. Dis.* **1,** e114
2. Gardon, J., Gardon-Wendel, N., Demanga, N., Kamgno, J., Chippaux, J. P., and Boussinesq, M. (1997) Serious reactions after mass treatment of onchocerciasis with ivermectin in an area endemic for *Loa loa* infection. *Lancet* **350,** 18–22
3. McCall, J. W., Genchi, C., Kramer, L. H., Guerrero, J., and Venco, L. (2008) Heartworm disease in animals and humans. *Adv. Parasitol.* **66,** 193–285
4. Wahl, G., Achu-Kwi, M. D., Mbah, D., Dawa, O., and Renz, A. (1994) Bovine onchocercosis in north Cameroon. *Vet. Parasitol.* **52,** 297–311
5. Osei-Atweneboana, M. Y., Eng, J. K., Boakye, D. A., Gyapong, J. O., and Prichard, R. K. (2007) Prevalence and intensity of *Onchocerca volvulus* infection and efficacy of ivermectin in endemic communities in Ghana: a two-phase epidemiological study. *Lancet* **369,** 2021–2029
6. Bourguinat, C., Keller, K., Bhan, A., Peregrine, A., Geary, T., and Prichard, R. (2011) Macrocyclic lactone resistance in *Dirofilaria immitis*. *Vet. Parasitol.* **181,** 388–392
7. Morris, C. P., Evans, H., Larsen, S. E., and Mitre, E. (2013) A comprehensive, model-based review of vaccine and repeat infection trials for filariasis. *Clin. Microbiol. Rev.* **26,** 381–421
8. Tamarozzi, F., Halliday, A., Gentil, K., Hoerauf, A., Pearlman, E., and Taylor, M. J. (2011) Onchocerciasis: the role of *Wolbachia* bacterial endosymbionts in parasite biology, disease pathogenesis, and treatment. *Clin. Microbiol. Rev.* **24,** 459–468
9. Ghedin, E., Wang, S., Spiro, D., Caler, E., Zhao, Q., Crabtree, J., Allen, J. E., Delcher, A. L., Guiliano, D. B., Miranda-Saavedra, D., Angiuoli, S. V., Creasy, T., Amedeo, P., Haas, B., El-Sayed, N. M., Wortman, J. R., Feldblyum, T., Tallon, L., Schatz, M., Shumway, M., Koo, H., Salzberg, S. L., Schobel, S., Pertea, M., Pop, M., White, O., Barton, G. J., Carlow, C. K., Crawford, M. J., Daub, J., Dimmic, M. W., Estes, C. F., Foster, J. M., Ganatra, M., Gregory, W. F., Johnson, N. M., Jin, J., Komuniecki, R., Korf, I., Kumar, S., Laney, S., Li, B. W., Li, W., Lindblom, T. H., Lustigman, S., Ma, D., Maina, C. V., Martin, D. M., McCarter, J. P., McReynolds, L., Mitreva, M., Nutman, T. B., Parkinson, J., Peregrin-Alvarez, J. M., Poole, C., Ren, Q., Saunders, L., Sluder, A. E., Smith, K., Stanke, M., Unnasch, T. R., Ware, J., Wei, A. D., Weil, G., Williams, D. J., Zhang, Y., Williams, S. A., Fraser-Liggett, C., Slatko, B., Blaxter, M. L., and Scott, A. L. (2007) Draft genome of the filarial nematode parasite *Brugia malayi*. *Science* **317,** 1756–1760
10. Godel, C., Kumar, S., Koutsovoulos, G., Ludin, P., Nilsson, D., Comandatore, F., Wrobel, N., Thompson, M., Schmid, C. D., Goto, S., Bringaud, F., Wolstenholme, A., Bandi, C., Epe, C., Kaminsky, R., Blaxter, M., and Maser, P. (2012) The genome of the heartworm, *Dirofilaria immitis*, reveals drug and vaccine targets. *FASEB J.* **26,** 4650–4661
11. Desjardins, C. A., Cerqueira, G. C., Goldberg, J. M., Dunning Hotopp, J. C., Haas, B. J., Zucker, J., Ribeiro, J. M., Saif, S., Levin, J. Z., Fan, L., Zeng, Q., Russ, C., Wortman, J. R., Fink, D. L., Birren, B. W., and Nutman, T. B. (2013) Genomics of *Loa loa*, a *Wolbachia*-free filarial parasite of humans. *Nat. Genet.* **45,** 495–500
12. Foster, J., Ganatra, M., Kamal, I., Ware, J., Makarova, K., Ivanova, N., Bhattacharyya, A., Kapatral, V., Kumar, S., Posfai, J., Vincze, T., Ingram, J., Moran, L., Lapidus, A., Omelchenko, M., Kyrpides, N., Ghedin, E., Wang, S., Goltsman, E., Joukov, V., Ostrovskaya, O., Tsukerman, K., Mazur, M., Comb, D., Koonin, E., and Slatko, B. (2005) The *Wolbachia* genome of *Brugia malayi*: endosymbiont evolution within a human pathogenic nematode. *PLoS Biol.* **3,** e121
13. Darby, A. C., Armstrong, S. D., Bah, G. S., Kaur, G., Hughes, M. A., Kay, S. M., Koldkjaer, P., Rainbow, L., Radford, A. D., Blaxter, M. L., Tanya, V. N., Trees, A. J., Cordaux, R., Wastling, J. M., and Makepeace, B. L. (2012) Analysis of gene expression from the *Wolbachia* genome of a filarial nematode supports both metabolic and defensive roles within the symbiosis. *Genome Res.* **22,** 2467–2477
14. Hewitson, J. P., Harcus, Y. M., Curwen, R. S., Dowle, A. A., Atmadja, A. K., Ashton, P. D., Wilson, A., and Maizels, R. M. (2008) The secretome of the filarial parasite, *Brugia malayi*: proteomic profile of adult excretory-secretory products. *Mol. Biochem. Parasitol.* **160,** 8–21
15. Bennuru, S., Meng, Z., Ribeiro, J. M., Semnani, R. T., Ghedin, E., Chan, K., Lucas, D. A., Veenstra, T. D., and Nutman, T. B. (2011) Stage-specific proteomic expression patterns of the human filarial parasite *Brugia malayi* and its endosymbiont *Wolbachia*. *Proc. Natl. Acad. Sci. U. S. A.* **108,** 9649–9654
16. Moreno, Y., and Geary, T. G. (2008) Stage- and gender-specific proteomic analysis of *Brugia malayi* excretory-secretory products. *PLoS Negl. Trop. Dis.* **2,** e326
17. Bennuru, S., Semnani, R., Meng, Z., Ribeiro, J. M., Veenstra, T. D., and Nutman, T. B. (2009) *Brugia malayi* excreted/secreted proteins at the host/parasite interface: stage- and gender-specific proteomic profiling. *PLoS Negl. Trop. Dis.* **3,** e410
18. Petit, G., Diagne, M., Marechal, P., Owen, D., Taylor, D., and Bain, O. (1992) Maturation of the filaria *Litomosoides sigmodontis* in BALB/c mice; comparative susceptibility of nine other inbred strains. *Ann. Parasitol. Hum. Comp.* **67,** 144–150
19. Bain, O., Petit, G., and Diagne, M. (1989) [*Litomosoides*, parasites of rodents; taxonomic consequences]. *Ann. Parasitol. Hum. Comp.* **64,** 268–289
20. Hoffmann, W., Petit, G., Schulz-Key, H., Taylor, D., Bain, O., and LeGoff, L. (2000) *Litomosoides sigmodontis* in mice: reappraisal of an old model for filarial research. *Parasitol. Today* **16,** 387–389
21. Pfaff, A. W., Schulz-Key, H., Soboslay, P. T., Taylor, D. W., MacLennan, K., and Hoffmann, W. H. (2002) *Litomosoides sigmodontis* cystatin acts as an immunomodulator during experimental filariasis. *Int. J. Parasitol.* **32,** 171–178
22. Taylor, M. D., LeGoff, L., Harris, A., Malone, E., Allen, J. E., and Maizels, R. M. (2005) Removal of regulatory T cell activity reverses hyporesponsiveness and leads to filarial parasite clearance *in vivo*. *J. Immunol.* **174,** 4924–4933
23. Hubner, M. P., Shi, Y., Torrero, M. N., Mueller, E., Larson, D., Soloviova, K., Gondorf, F., Hoerauf, A., Killoran, K. E., Stocker, J. T., Davies, S. J., Tarbell, K. V., and Mitre, E. (2012) Helminth protection against autoimmune diabetes in nonobese diabetic mice is independent of a type 2 immune shift and requires TGF-beta. *J. Immunol.* **188,** 559–568
24. LeGoff, L., Martin, C., Oswald, I. P., Vuong, P. N., Petit, G., Ungeheuer, M. N., and Bain, O. (2000) Parasitology and immunology of mice vaccinated with irradiated *Litomosoides sigmodontis* larvae. *Parasitology* **120,** 271–280
25. Babayan, S. A., Luo, H., Gray, N., Taylor, D. W., and Allen, J. E. (2012) Deletion of parasite immune modulatory sequences combined with immune activating signals enhances vaccine mediated protection against filarial nematodes. *PLoS Negl. Trop. Dis.* **6,** e1968
26. Comandatore, F., Sassera, D., Montagna, M., Kumar, S., Koutsovoulos, G., Thomas, G., Repton, C., Babayan, S. A., Gray, N., Cordaux, R., Darby, A., Makepeace, B., and Blaxter, M. (2013) Phylogenomics and analysis of shared genes suggest a single transition to mutualism in *Wolbachia* of nematodes. *Genome Biol. Evol.* **5,** 1668–1674
27. Schwanhausser, B., Busse, D., Li, N., Dittmar, G., Schuchhardt, J., Wolf, J., Chen, W., and Selbach, M. (2011) Global quantification of mamma-

lian gene expression control. *Nature* **473,** 337–342
28. Vizcaino, J. A., Cote, R. G., Csordas, A., Dianes, J. A., Fabregat, A., Foster, J. M., Griss, J., Alpi, E., Birim, M., Contell, J., O'Kelly, G., Schoenegger, A., Ovelleiro, D., Perez-Riverol, Y., Reisinger, F., Rios, D., Wang, R., and Hermjakob, H. (2013) The PRoteomics IDEntifications (PRIDE) database and associated tools: status in 2013. *Nucleic Acids Res.* **41,** D1063–D1069
29. R Development Core Team. (2013) *R: A Language and Environment for Statistical Computing*, The R Foundation for Statistical Computing, Vienna, Austria
30. Benjamini, Y., and Hochberg, Y. (1995) Controlling the false discovery rate - A practical and powerful approach to multiple testing. *J. R. Stat. Soc. Ser. B* **57,** 289–300
31. Kelley, L. A., and Sternberg, M. J. (2009) Protein structure prediction on the Web: a case study using the Phyre server. *Nat. Protoc.* **4,** 363–371
32. Quevillon, E., Silventoinen, V., Pillai, S., Harte, N., Mulder, N., Apweiler, R., and Lopez, R. (2005) InterProScan: protein domains identifier. *Nucleic Acids Res.* **33,** W116–W120
33. Martin, B., Chadwick, W., Yi, T., Park, S. S., Lu, D., Ni, B., Gadkaree, S., Farhang, K., Becker, K. G., and Maudsley, S. (2012) VENNTURE–a novel Venn diagram investigational tool for multiple pharmacological dataset analysis. *PLoS One* **7,** e36911
34. Petersen, T. N., Brunak, S., von, H. G., and Nielsen, H. (2011) SignalP 4.0: discriminating signal peptides from transmembrane regions. *Nat. Methods* **8,** 785–786
35. Bendtsen, J. D., Jensen, L. J., Blom, N., von, H. G., and Brunak, S. (2004) Feature-based prediction of non-classical and leaderless protein secretion. *Protein Eng. Des. Sel.* **17,** 349–356
36. Claros, M. G., and Vincens, P. (1996) Computational method to predict mitochondrially imported proteins and their targeting sequences. *Eur. J. Biochem.* **241,** 779–786
37. Steentoft, C., Vakhrushev, S. Y., Joshi, H. J., Kong, Y., Vester-Christensen, M. B., Schjoldager, K. T., Lavrsen, K., Dabelsteen, S., Pedersen, N. B., Marcos-Silva, L., Gupta, R., Bennett, E. P., Mandel, U., Brunak, S., Wandall, H. H., Levery, S. B., and Clausen, H. (2013) Precision mapping of the human O-GalNAc glycoproteome through SimpleCell technology. *EMBO J.* **32,** 1478–1488
38. Duckert, P., Brunak, S., and Blom, N. (2004) Prediction of proprotein convertase cleavage sites. *Protein Eng. Des. Sel.* **17,** 107–112
39. Jex, A. R., Liu, S., Li, B., Young, N. D., Hall, R. S., Li, Y., Yang, L., Zeng, N., Xu, X., Xiong, Z., Chen, F., Wu, X., Zhang, G., Fang, X., Kang, Y., Anderson, G. A., Harris, T. W., Campbell, B. E., Vlaminck, J., Wang, T., Cantacessi, C., Schwarz, E. M., Ranganathan, S., Geldhof, P., Nejsum, P., Sternberg, P. W., Yang, H., Wang, J., Wang, J., and Gasser, R. B. (2011) *Ascaris suum* draft genome. *Nature* **479,** 529–533
40. Sievers, F., and Higgins, D. G. (2014) Clustal Omega, accurate alignment of very large numbers of sequences. *Methods Mol. Biol.* **1079,** 105–116
41. Ronquist, F., Teslenko, M., van der Mark, P., Ayres, D. L., Darling, A., Hohna, S., Larget, B., Liu, L., Suchard, M. A., and Huelsenbeck, J. P. (2012) MrBayes 3.2: efficient Bayesian phylogenetic inference and model choice across a large model space. *Syst. Biol.* **61,** 539–542
42. Crooks, G. E., Hon, G., Chandonia, J. M., and Brenner, S. E. (2004) WebLogo: a sequence logo generator. *Genome Res.* **14,** 1188–1190
43. Lustigman, S., Brotman, B., Huima, T., Prince, A. M., and McKerrow, J. H. (1992) Molecular cloning and characterization of onchocystatin, a cysteine proteinase inhibitor of *Onchocerca volvulus*. *J. Biol. Chem.* **267,** 17339–17346
44. Liebau, E., Hoppner, J., Muhlmeister, M., Burmeister, C., Luersen, K., Perbandt, M., Schmetz, C., Buttner, D., and Brattig, N. (2008) The secretory omega-class glutathione transferase OvGST3 from the human pathogenic parasite *Onchocerca volvulus*. *FEBS J.* **275,** 3438–3453
45. Scott, A. L., Dinman, J., Sussman, D. J., and Ward, S. (1989) Major sperm protein and actin genes in free-living and parasitic nematodes. *Parasitology* **98,** 471–478
46. Zahner, H., Hobom, G., and Stirm, S. (1995) The microfilarial sheath and its proteins. *Parasitol. Today* **11,** 116–120
47. Willenbucher, J., Hofle, W., and Lucius, R. (1993) The filarial antigens Av33/Ov33–3 show striking similarities to the major pepsin inhibitor from *Ascaris suum*. *Mol. Biochem. Parasitol.* **57,** 349–351
48. Harnett, W., Houston, K. M., Tate, R., Garate, T., Apfel, H., Adam, R., Haslam, S. M., Panico, M., Paxton, T., Dell, A., Morris, H., and Brzeski, H. (1999) Molecular cloning and demonstration of an aminopeptidase activity in a filarial nematode glycoprotein. *Mol. Biochem. Parasitol.* **104,** 11–23
49. Ao, J. Q., Ling, E., Rao, X. J., and Yu, X. Q. (2008) A novel ML protein from *Manduca sexta* may function as a key accessory protein for lipopolysaccharide signaling. *Mol. Immunol.* **45,** 2772–2781
50. Storch, J., and Xu, Z. (2009) Niemann-Pick C2 (NPC2) and intracellular cholesterol trafficking. *Biochim. Biophys. Acta* **1791,** 671–678
51. Erttmann, K. D., and Gallin, M. Y. (1996) Onchocerca volvulus: identification of cDNAs encoding a putative phosphatidyl-ethanolamine-binding protein and a putative partially processed mRNA precursor. *Gene* **174,** 203–207
52. Gallin, M. Y., Tan, M., Kron, M. A., Rechnitzer, D., Greene, B. M., Newland, H. S., White, A. T., Taylor, H. R., and Unnasch, T. R. (1989) *Onchocerca volvulus* recombinant antigen: physical characterization and clinical correlates with serum reactivity. *J. Infect. Dis.* **160,** 521–529
53. Dissanayake, S., Xu, M., and Piessens, W. F. (1992) A cloned antigen for serological diagnosis of *Wuchereria bancrofti* microfilaremia with daytime blood samples. *Mol. Biochem. Parasitol.* **56,** 269–277
54. Hunter, S. J., Thompson, F. J., Tetley, L., and Devaney, E. (2001) Temperature is a cue for gene expression in the post-infective L3 of the parasitic nematode *Brugia pahangi*. *Mol. Biochem. Parasitol.* **112,** 1–9
55. Gare, D., Boyd, J., and Connolly, B. (2004) Developmental regulation and secretion of nematode-specific cysteine-glycine domain proteins in *Trichinella spiralis*. *Mol. Biochem. Parasitol.* **134,** 257–266
56. Makinen, P. L., and Makinen, K. K. (1981) Purification and properties of rat skin acid phosphatases. *Int. J. Pept. Protein Res.* **18,** 352–369
57. Fukushige, T., Goszczynski, B., Yan, J., and McGhee, J. D. (2005) Transcriptional control and patterning of the *pho-1* gene, an essential acid phosphatase expressed in the *C. elegans* intestine. *Dev. Biol.* **279,** 446–461
58. Grant, R. P., Buttery, S. M., Ekman, G. C., Roberts, T. M., and Stewart, M. (2005) Structure of MFP2 and its function in enhancing MSP polymerization in *Ascaris* sperm amoeboid motility. *J. Mol. Biol.* **347,** 583–595
59. Ou, X., Tang, L., McCrossan, M., Henkle-Dührsen, K., and Selkirk, M. E. (1995) *Brugia malayi*: localisation and differential expression of extracellular and cytoplasmic CuZn superoxide dismutases in adults and microfilariae. *Exp. Parasitol.* **80,** 515–529
60. Ford, L., Guiliano, D. B., Oksov, Y., Debnath, A. K., Liu, J., Williams, S. A., Blaxter, M. L., and Lustigman, S. (2005) Characterization of a novel filarial serine protease inhibitor, Ov-SPI-1, from *Onchocerca volvulus*, with potential multifunctional roles during development of the parasite. *J. Biol. Chem.* **280,** 40845–40856
61. Frank, G. R., Wisnewski, N., Brandt, K. S., Carter, C. R., Jennings, N. S., and Selkirk, M. E. (1999) Molecular cloning of the 22–24 kDa excretory-secretory 22U protein of *Dirofilaria immitis* and other filarial nematode parasites. *Mol. Biochem. Parasitol.* **98,** 297–302
62. Gnanasekar, M., Padmavathi, B., and Ramaswamy, K. (2005) Cloning and characterization of a novel immunogenic protein 3 (NIP3) from *Brugia malayi* by immuno screening of a phage-display cDNA expression library. *Parasitol. Res*. **97,** 49–58
63. Chu, D. S., Liu, H., Nix, P., Wu, T. F., Ralston, E. J., Yates, J. R., 3rd, and Meyer, B. J. (2006) Sperm chromatin proteomics identifies evolutionarily conserved fertility factors. *Nature* **443,** 101–105
64. Blaxter, M. (1998) *Caenorhabditis elegans* is a nematode. *Science* **282,** 2041–2046
65. Beeton, C., Pennington, M. W., and Norton, R. S. (2011) Analogs of the sea anemone potassium channel blocker ShK for the treatment of autoimmune diseases. *Inflamm. Allergy Drug Targets.* **10,** 313–321
66. Loukas, A., Hintz, M., Linder, D., Mullin, N. P., Parkinson, J., Tetteh, K. K., and Maizels, R. M. (2000) A family of secreted mucins from the parasitic nematode *Toxocara canis* bears diverse mucin domains but shares similar flanking six-cysteine repeat motifs. *J. Biol. Chem.* **275,** 39600–39607
67. Yamaguchi, Y., Hasegawa, Y., Honma, T., Nagashima, Y., and Shiomi, K. (2010) Screening and cDNA cloning of Kv1 potassium channel toxins in sea anemones. *Mar. Drugs* **8,** 2893–2905
68. Blaxter, M. L., and Robertson, W. M. (1998) The cuticle, In: Perry, R. N., and Wright, D. J. (eds), *The physiology and biochemistry of free-living and plant-parasitic nematodes*, pp. 25–48, CABI Publishing, Walling-

ford, Oxon
69. Yegutkin, G. G. (2008) Nucleotide- and nucleoside-converting ectoenzymes: important modulators of purinergic signalling cascade. *Biochim. Biophys. Acta* **1783,** 673–694
70. Peerschke, E. I., and Ghebrehiwet, B. (2007) The contribution of gC1qR/p33 in infection and inflammation. *Immunobiology* **212,** 333–342
71. Irvine, M., Huima, T., Prince, A. M., and Lustigman, S. (1994) Identification and characterization of an *Onchocerca volvulus* cDNA clone encoding a highly immunogenic calponin-like protein. *Mol. Biochem. Parasitol.* **65,** 135–146
72. Wilson, W. R., Tuan, R. S., Shepley, K. J., Freedman, D. O., Greene, B. M., Awadzi, K., and Unnasch, T. R. (1994) The *Onchocerca volvulus* homologue of the multifunctional polypeptide protein disulfide isomerase. *Mol. Biochem. Parasitol.* **68,** 103–117
73. Mancuso, V. P., Parry, J. M., Storer, L., Poggioli, C., Nguyen, K. C., Hall, D. H., and Sundaram, M. V. (2012) Extracellular leucine-rich repeat proteins are required to organize the apical extracellular matrix and maintain epithelial junction integrity in *C. elegans. Development* **139,** 979–990
74. Lu, W., Egerton, G. L., Bianco, A. E., and Williams, S. A. (1998) Thioredoxin peroxidase from *Onchocerca volvulus*: a major hydrogen peroxide detoxifying enzyme in filarial parasites. *Mol. Biochem. Parasitol.* **91,** 221–235
75. Geary, J., Satti, M., Moreno, Y., Madrill, N., Whitten, D., Headley, S. A., Agnew, D., Geary, T., and Mackenzie, C. (2012) First analysis of the secretome of the canine heartworm, *Dirofilaria immitis. Parasit. Vectors* **5,** 140
76. Babayan, S. A., Allen, J. E., and Taylor, D. W. (2012) Future prospects and challenges of vaccines against filariasis. *Parasite Immunol.* **34,** 243–253
77. Sepsenwol, S., and Taft, S. J. (1990) *In vitro* induction of crawling in the amoeboid sperm of the nematode parasite, *Ascaris suum. Cell Motil. Cytoskeleton* **15,** 99–110
78. Morgan, K. L., Estevez, A. O., Mueller, C. L., Cacho-Valadez, B., Miranda-Vizuete, A., Szewczyk, N. J., and Estevez, M. (2010) The glutaredoxin GLRX-21 functions to prevent selenium-induced oxidative stress in *Caenorhabditis elegans. Toxicol. Sci.* **118,** 530–543
79. Hawkes, W. C., and Turek, P. J. (2001) Effects of dietary selenium on sperm motility in healthy men. *J. Androl.* **22,** 764–772
80. Zhao, Y., Sun, W., Zhang, P., Chi, H., Zhang, M. J., Song, C. Q., Ma, X., Shang, Y., Wang, B., Hu, Y., Hao, Z., Huhmer, A. F., Meng, F., L'hernault, S. W., He, S. M., Dong, M. Q., and Miao, L. (2012) Nematode sperm maturation triggered by protease involves sperm-secreted serine protease inhibitor (Serpin). *Proc. Natl. Acad. Sci. U. S. A.* **109,** 1542–1547
81. Johnson, M. H., Orihel, T. C., and Beaver, P. C. (1974) *Dipetalonema viteae* in the experimentally infected jird, *Meriones unguiculatus.* I. Insemination, development from egg to microfilaria, reinsemination, and longevity of mated and unmated worms. *J. Parasitol.* **60,** 302–309
82. Funato, Y., and Miki, H. (2007) Nucleoredoxin, a novel thioredoxin family member involved in cell growth and differentiation. *Antioxid. Redox. Signal.* **9,** 1035–1057
83. Kunchithapautham, K., Padmavathi, B., Narayanan, R. B., Kaliraj, P., and Scott, A. L. (2003) Thioredoxin from *Brugia malayi*: defining a 16-kilodalton class of thioredoxins from nematodes. *Infect. Immun.* **71,** 4119–4126
84. Gems, D., and Riddle, D. L. (1996) Longevity in *Caenorhabditis elegans* reduced by mating but not gamete production. *Nature* **379,** 723–725
85. Kumari, S., Lillibridge, C. D., Bakeer, M., Lowrie, R. C., Jr., Jayaraman, K., and Philipp, M. T. (1994) *Brugia malayi*: the diagnostic potential of recombinant excretory/secretory antigens. *Exp. Parasitol.* **79,** 489–505
86. Bi, M., Hickox, J. R., Winfrey, V. P., Olson, G. E., and Hardy, D. M. (2003) Processing, localization and binding activity of zonadhesin suggest a function in sperm adhesion to the zona pellucida during exocytosis of the acrosome. *Biochem. J.* **375,** 477–488
87. Heiman, M. G., and Shaham, S. (2009) DEX-1 and DYF-7 establish sensory dendrite length by anchoring dendritic tips during cell migration. *Cell* **137,** 344–355
88. Matyash, V., Geier, C., Henske, A., Mukherjee, S., Hirsh, D., Thiele, C., Grant, B., Maxfield, F. R., and Kurzchalia, T. V. (2001) Distribution and transport of cholesterol in *Caenorhabditis elegans. Mol. Biol. Cell* **12,** 1725–1736
89. Moreno, Y., Gros, P. P., Tam, M., Segura, M., Valanparambil, R., Geary, T. G., and Stevenson, M. M. (2011) Proteomic analysis of excretory-secretory products of *Heligmosomoides polygyrus* assessed with next-generation sequencing transcriptomic information. *PLoS Negl. Trop. Dis.* **5,** e1370
90. Nagaraj, S. H., Gasser, R. B., and Ranganathan, S. (2008) Needles in the EST haystack: large-scale identification and analysis of excretory-secretory (ES) proteins in parasitic nematodes using expressed sequence tags (ESTs). *PLoS Negl. Trop. Dis.* **2,** e301
91. Kang, Y., Zhao, D., Liang, H., Liu, B., Zhang, Y., Liu, Q., Wang, X., and Liu, Y. (2012) Structural study of TTR-52 reveals the mechanism by which a bridging molecule mediates apoptotic cell engulfment. *Genes Dev.* **26,** 1339–1350
92. Jacob, J., Vanholme, B., Haegeman, A., and Gheysen, G. (2007) Four transthyretin-like genes of the migratory plant-parasitic nematode *Radopholus similis*: members of an extensive nematode-specific family. *Gene* **402,** 9–19
93. Saverwyns, H., Visser, A., Van, Durme, J., Power, D., Morgado, I., Kennedy, M. W., Knox, D. P., Schymkowitz, J., Rousseau, F., Gevaert, K., Vercruysse, J., Claerebout, E., and Geldhof, P. (2008) Analysis of the transthyretin-like (TTL) gene family in *Ostertagia ostertagi*–comparison with other strongylid nematodes and *Caenorhabditis elegans. Int. J. Parasitol.* **38,** 1545–1556
94. Landmann, F., Foster, J. M., Slatko, B. E., and Sullivan, W. (2012) Efficient *in vitro* RNA interference and immunofluorescence-based phenotype analysis in a human parasitic nematode, *Brugia malayi. Parasit. Vectors* **5,** 16
95. Wergin, W. P., and Endo, B. Y. (1976) Ultrastructure of a neurosensory organ in a root-knot nematode. *J. Ultrastruct. Res.* **56,** 258–276
96. Madathiparambil, M. G., Kaleysa, K. N., and Raghavan, K. (2009) A diagnostically useful 200-kDa protein is secreted through the surface pores of the filarial parasite *Setaria digitata. Parasitol. Res.* **105,** 1099–1104
97. Kolotuev, I., Apaydin, A., and Labouesse, M. (2009) Secretion of Hedgehog-related peptides and WNT during *Caenorhabditis elegans* development. *Traffic.* **10,** 803–810
98. Prusse, A., Vollmer, S., and Diesfeld, H. J. (1983) Immunocytochemical and ultrastructural studies on *Dipetalonema viteae* (Filarioidea). *J. Helminthol.* **57,** 127–142
99. Kozek, W. J. (2005) What is new in the *Wolbachia*/*Dirofilaria* interaction? *Vet. Parasitol.* **133,** 127–132
100. Brattig, N. W., Bazzocchi, C., Kirschning, C. J., Reiling, N., Büttner, D. W., Ceciliani, F., Geisinger, F., Hochrein, H., Ernst, M., Wagner, H., Bandi, C., and Hoerauf, A. (2004) The major surface protein of *Wolbachia* endosymbionts in filarial nematodes elicits immune responses through TLR2 and TLR4. *J. Immunol.* **173,** 437–445
101. Landmann, F., Foster, J. M., Slatko, B., and Sullivan, W. (2010) Asymmetric *Wolbachia* segregation during early *Brugia malayi* embryogenesis determines its distribution in adult host tissues. *PLoS Negl. Trop. Dis.* **4,** e758
102. Melnikow, E., Xu, S., Liu, J., Li, L., Oksov, Y., Ghedin, E., Unnasch, T. R., and Lustigman, S. (2011) Interaction of a *Wolbachia* WSP-like protein with a nuclear-encoded protein of *Brugia malayi. Int. J. Parasitol.* **41,** 1053–1061
103. Henderson, B., and Martin, A. (2011) Bacterial virulence in the moonlight: multitasking bacterial moonlighting proteins are virulence determinants in infectious disease. *Infect. Immun.* **79,** 3476–3491
104. Hansen, R. D., Trees, A. J., Bah, G. S., Hetzel, U., Martin, C., Bain, O., Tanya, V. N., and Makepeace, B. L. (2011) A worm's best friend: recruitment of neutrophils by *Wolbachia* confounds eosinophil degranulation against the filarial nematode *Onchocerca ochengi. Proc. R. Soc. B* **278,** 2293–2302
105. Argueta, J. G., Shiota, S., Yamaguchi, N., Masuhiro, Y., and Hanazawa, S. (2006) Induction of *Porphyromonas gingivalis* GroEL signaling via binding to Toll-like receptors 2 and 4. *Oral Microbiol. Immunol.* **21,** 245–251
106. Suba, N., Shiny, C., Taylor, M. J., and Narayanan, R. B. (2007) *Brugia malayi Wolbachia* HSP60 IgG antibody and isotype reactivity in different clinical groups infected or exposed to human bancroftian lymphatic filariasis. *Exp. Parasitol.* **116,** 291–295
107. Storey, D. M., and Al-Mukhtar, A. S. (1982) Vaccination of Jirds, *Meriones unguiculatus*, against *Litomosoides carinii* and *Brugia pahangi* using irradiate larvae of *L. carinii. Tropenmed. Parasitol.* **33,** 23–24

108. Babayan, S. A., Attout, T., Harris, A., Taylor, M. D., Le, Goff, L., Vuong, P. N., Renia, L., Allen, J. E., and Bain, O. (2006) Vaccination against filarial nematodes with irradiated larvae provides long-term protection against the third larval stage but not against subsequent life cycle stages. *Int. J. Parasitol.* **36,** 903–914
109. Allen, J. E., Daub, J., Guiliano, D., McDonnell, A., Lizotte-Waniewski, M., Taylor, D. W., and Blaxter, M. (2000) Analysis of genes expressed at the infective larval stage validates utility of *Litomosoides sigmodontis* as a murine model for filarial vaccine development. *Infect. Immun.* **68,** 5454–5458
110. Makepeace, B. L., Jensen, S. A., Laney, S. J., Nfon, C. K., Njongmeta, L. M., Tanya, V. N., Williams, S. A., Bianco, A. E., and Trees, A. J. (2009) Immunisation with a multivalent, subunit vaccine reduces patent infection in a natural bovine model of onchocerciasis during intense field exposure. *PLoS Negl. Trop. Dis.* **3,** e544
111. Ziewer, S., Hubner, M. P., Dubben, B., Hoffmann, W. H., Bain, O., Martin, C., Hoerauf, A., and Specht, S. (2012) Immunization with *L. sigmodontis* microfilariae reduces peripheral microfilaraemia after challenge infection by inhibition of filarial embryogenesis. *PLoS Negl. Trop. Dis.* **6,** e1558
112. Townson, S., and Bianco, A. E. (1982) Immunization of calves against the microfilariae of *Onchocerca lienalis. J. Helminthol.* **56,** 297–303
113. Hoffmann, W. H., Pfaff, A. W., Schulz-Key, H., Soboslay, P. T., and Soboslav, P. T. (2001) Determinants for resistance and susceptibility to microfilaraemia in *Litomosoides sigmodontis* filariasis. *Parasitology* **122,** 641–649
114. Hashmi, S., Zhang, J., Oksov, Y., Ji, Q., and Lustigman, S. (2006) The *Caenorhabditis elegans* CPI-2a cystatin-like inhibitor has an essential regulatory role during oogenesis and fertilization. *J. Biol. Chem.* **281,** 28415–28429